Energy Harvesting for Remote Monitoring of Environmental Applications

Panu Thainiramit

A Thesis Submitted in Partial Fulfillment of the Requirements for the Degree of Doctor of Philosophy in Environmental Management

Prince of Songkla University

2019

Energy Harvesting for Remote Monitoring of Environmental Applications

Panu Thainiramit

A Thesis Submitted in Partial Fulfillment of the Requirements for the Degree of Doctor of Philosophy in Environmental Management

Prince of Songkla University

2019

Thesis Title	Energy Harvesting for Remote Monitoring of Environmental Applications
Author	Mr. Panu Thainiramit
Major Program	Environmental Management

Major Advisor

.....
(Assoc. Prof. Dr. Nantakan Muensit)

Co-advisor :

.....
(Asst. Prof. Dr. Kua-Anan Techato)

.....
(Assoc. Prof. Dr. Yufridin Bin Wahab)

Examining Committee :

.....Chairperson
(Asst. Prof. Dr. Don Isarakorn)

.....Committee
(Assoc. Prof. Dr. Pruittikorn Smithmaitrie)

.....Committee
(Asst. Prof. Dr. Chaiwat Rongsayamanont)

.....Committee
(Assoc. Prof. Dr. Nantakan Muensit)

.....Committee
(Asst. Prof. Dr. Kua-Anan Techato)

The Graduate School, Prince of Songkla University, has approved this thesis as partial fulfillment of the requirements for the Doctor of Philosophy Degree in Environmental Management.

.....
(Prof. Dr. Damrongsak Faroongsarng)
Dean of Graduate School

This is to certify that the work here submitted is the result of the candidate's own investigations. Due acknowledgement has been made of any assistance received.

.....Signature
(Assoc. Prof. Dr. Nantakan Muensit)
Major Advisor

.....Signature
(Asst. Prof. Dr. Kua-Anan Techato)
Co-advisor

.....Signature
(Assoc. Prof. Dr. Yufridin Bin Wahab)
Co-advisor

.....Signature
(Mr. Panu Thainiramit)
Candidate

I hereby certify that this work has not been accepted in substance for any degree, and is not being currently submitted in candidature for any degree.

.....Signature

(Mr. Panu Thainiramit)

Candidate

ชื่อวิทยานิพนธ์ การเก็บเกี่ยวพลังงานสำหรับระบบเฝ้าระวังระยะไกลเพื่อการประยุกต์ในงานด้านสิ่งแวดล้อม

ผู้เขียน นายภาณุ ไทยนิรมิตร

สาขา การจัดการสิ่งแวดล้อม

ปีการศึกษา 2561

บทคัดย่อ

ที่พักอาศัยมีจำนวนเพิ่มขึ้นอย่างรวดเร็วในหลาย ๆ ประเทศ มาพร้อมกับความต้องการความสะดวกสบายด้วยข้าวของเครื่องใช้และเทคโนโลยีที่ก้าวเข้ามาเป็นส่วนหนึ่งของการดำเนินชีวิตประจำวันอย่างขาดมิได้ งานวิจัยนี้ได้แสดงให้เห็นว่าอุปกรณ์สื่อสารไร้สายที่สามารถทำงานแบบอิสระโดยอาศัยอุปกรณ์รับสัญญาณซึ่งใช้สัญญาณไฟฟ้าจากแหล่งกำเนิดไฟฟ้าด้วยหลักการทางไพอิโซอิเล็กทริกชนิดเซรามิกเป็นอุปกรณ์เพื่อเปลี่ยนพลังงานกลเป็นไฟฟ้า ที่ติดตั้งอยู่บนโครงสร้างอย่างง่ายแบบบีมเพื่อดักจับพลังงานสั่นที่ได้จากคอมเพรสเซอร์ของเครื่องปรับอากาศที่ใช้งานกันอยู่ทั่วไปที่ความถี่ทำงานซึ่งออกแบบบีมให้ทำงานได้ใกล้เคียงกับความถี่จากแหล่งกำเนิด พลังงานไฟฟ้าที่ได้สามารถเก็บสะสมในตัวเก็บประจุโดยปราศจากวงจรควบคุมแรงดันเพื่อเพิ่มความสามารถในการประจุกระแสไฟฟ้าเข้าสู่ตัวเก็บประจุแต่อย่างใด อีกทั้งพลังงานไฟฟ้าที่ได้ยังสามารถนำไปใช้งานกับอุปกรณ์สื่อสารไร้สายที่ทำหน้าที่เป็นตัวรับสัญญาณจากตัวส่งสัญญาณที่ได้รับกระแสไฟฟ้าจากที่สะสมไว้โดยถูกควบคุมการคายกระแสไฟฟ้าด้วยสวิตช์อิเล็กทรอนิกส์ ผลศึกษาแสดงให้เห็นว่าหากมีขนาดการสั่นเพียงพอที่เป็นค่าเริ่มต้นของค่าคุณภาพหลังจากกำลังไฟฟ้าเข้าสู่ช่วงอิ่มตัว กล่าวคือประจุเริ่มต้นที่สามามาถจ่ายให้วงจรเพียงพอและมีประจุขั้นต่ำเริ่มต้นจากขาออกของวงจรควบคุมแรงดันทำให้สามารถประจุกระแสไฟฟ้าไปยังแบตเตอรี่ชนิดประจุซ้ำได้ขนาด 150 mAh ให้เต็มความจุได้ภายในเวลา 40 ชั่วโมง ในขณะที่การสั่นที่ได้จากเครื่องปรับอากาศไม่เพียงพอสำหรับการประจุแบตเตอรี่ เนื่องจากเป็นการสั่นที่มีค่าความเร่งการสั่นน้อยมาก ๆ เมื่อเทียบกับความต้องการของวงจร แม้กระนั้นก็ตามการสั่นน้อย ๆ นี้สามารถประจุให้ตัวเก็บประจุที่มีขนาด 3,150 μF จนได้รับประจุเต็มภายใน 1 ชั่วโมง ซึ่งความจุเพียงพอสำหรับอุปกรณ์รับสัญญาณแบบไร้สายที่รับค่าข้อมูล ได้แก่ อุณหภูมิ เป็นต้น ซึ่งเพียงพอสำหรับข้อมูลสภาพแวดล้อมภายนอกอาคารเพื่อการประมวลผลและใช้ประโยชน์ต่อไป

Thesis title Energy Harvesting for Remote Monitoring of Environmental Applications
Author Mr. Panu Thainiramit
Major Program Environmental Management
Academic Year 2018

ABSTRACT

The number of residential buildings in many countries around the world has been growing rapidly. Comfortable furniture and smart peripheral devices have become commonly used in daily life. This dissertation demonstrated a simple wireless standalone system for the case of the receiver attached to the compressor unit of the conventional air conditioner. The research proposed an air-compressor as a source of discrete excitation and employed a conventional buzzer as a transducer. The vibration is harvested as its mechanical energy to electricity by using a beam structure (cantilever beam) glued with the piezoelectric ceramic. The output energy stored in capacitors is consequent as a miniature generator. The transmitted data are then received a wireless receiver from the remote transmitter. Moreover, the potential result for charging the rechargeable battery appears to illustrate that the harvesting structure requires more electricity to consume the enhancement circuit by providing a high magnitude of vibrations following the threshold FoM parameter after saturated power ranges. As a result, the piezoelectric material generates a trickle current for charging the rechargeable battery, capacity 150 mAh, thus being fully charged within 40 hours. These results confirmed that the simple beam could act as a charger for the connected capacitors which were later an energy source to feed the wireless devices even though there is only a standard circuit by controlling the on/off state of a simple switch between the receiver module. In this research, a running air-conditioner generated a charging cycle to capacitors of 3,150 μF within 1 hour. It is truly enough to send and receive the data of ambient temperature around the building. This application is useful as a warning sign for inhabitants.

ACKNOWLEDGEMENTS

First and foremost, I would like to express my deepest appreciation and thanks to my supervisor, Associate Professor Dr. Nantakan Muensit, for her suggestion, encouragement, and supervision throughout my graduate studies; her tremendous instructions, mentoring, and complete support of my work and learning experience.

In addition, I would like to express my special appreciation and thanks to my co-supervisor, Assistant Professor Dr. Kua-Anan Techato, and Associate Professor Dr. Yufridin Bin Wahab, for his suggestion, encouraging my research and for allowing me to grow as a research scientist throughout my graduate studies.

My special thanks go to the Chairperson Assistant Professor Dr. Don Isarakorn, and Committee Member, Associate Professor Dr. Pruittikorn Smithmaitrie, and Assistant Professor Dr. Chaiwat Rongsayamanont for serving as my committee members even at hardship. I also want to thank you for letting my defense to be a valuable moment, and for your brilliant comments and suggestions, for taking time out of their busy schedules to evaluate my work.

I would never forget all my friends in the AMBIENCE Laboratory Malaysia, the Physics Workshop Office, and the Material Physics Laboratory as well as other laboratories, for their grateful helping hand.

Very important thanks go to my family, father, mother, aunt, and sister for their love, kindness and endless care which always affords me during education, and I would also like to thank my beloved wife. Thank you for supporting me for everything, and especially I cannot thank you enough for encouraging me throughout this experience.

Finally, I would like to acknowledge all financial support. Furthermore, my thanks and appreciations go to the Center of Excellence in Nanotechnology for Energy (CENE) and the Department of Environmental Management, Prince of Songkla University for providing me research equipment and many opportunities.

Panu Thainiramit

CONTENTS

LIST OF FIGURES

LIST OF TABLES

NOMENCLATURE AND ABBREVIATION

NOMENCLATURE

ω (corresponding to f)	Input angular frequency, (*Hz*)
ω_0 (corresponding to f_0)	Resonance angular frequency, (*Hz*)
ε_0	Permittivity of free space, (*F/m*)
ε_{33}	Permittivity, (*F/m*)
a_e	Area of electrode on piezoelectric element, (m^2)
C	Damping coefficient, (*N.s/m*)
C_f	Filter capacitance, (*F*)
c	Elastic stiffness constant, (N/m^2)
C_P	Capacitance of piezoelectric element, (*F*)
D (superscript)	Constant electrical displacement (at open circuit)
D	Electric displacement component, (C/m^2)
d	Piezoelectric constant, (*m/V, C/N*)
E (superscript)	Constant electric field (at short circuit)
E	Electric field component, (*V/m*)
e	Piezoelectric constant, (C/m^2)
H	Beam height, (*m*)
I	Current, (*A*)
k	Coupling factor, (-)
L	Inductance, (*H*)
l	Beam length, (*m*)
M	Mass, (*kg*)
K	Structural stiffness, (*N/m*)
P_{EH}	Harvested power, (*W*)
P	Polarization, (C/m^2)
Q_{str}	Structural quality factor, (-)
Q	Quality factor, (-)

R_L	Resistance, (Ω)
S (superscript)	Constant strain (at mechanical clamped)
S	Strain component, (-)
s	Elastic compliance constant, (m^2/N)
T (superscript)	Constant stress (at free-clamped mechanical)
T	Stress component, (N/m^2)
t_0	Thickness of Piezoelectric element, (m)
V_P	Piezoelectric voltage, (V)
W	Beam width, (m)
y	Displacement, (m)

ABBREVIATION

AC	Alternating Current
A/D	Analog to Digital Converter
DC	Direct Current
D/A	Digital to Analog Converter
WSD	Wireless Sensor Device or Node
WSN	Wireless Sensor Network
RF	Radio Frequency
GSM	Global System for Mobile Communications
SDOF	Single Degree of Freedom
VEH	Vibration Energy Harvesting
IC	Integrated Circuit
FoM	Figure of Merit

RESEARCH CONTRIBUTIONS

I. The modelling development of piezoelectric equations is to propose the stress and electric field parameters of the piezoelectric relations to predict and validate an electrical power based on a direct current term with respect to a quality factor. The quality factor is undergone by validating the theoretical demonstration as the controlled structural parameters linked to the damping factor and natural frequency of the harvesting structure. This dissertation undertakes the assumption that this modelling development seems likely to illustrate obviously the simple measured parameters leading to the equivalent circuit and mechanical model as the principle of the piezo-electromechanical model.

II. By applying a low-power system, the Piezoelectric Method is designed and employed as a robust technology of the vibration energy harvesting, that is suitable for the high impact used nowadays. The vibration energy harvesting using piezoelectric method is influenced by the specific demonstrations and installation areas for these system designs corresponding to discrete vibrational implementations. This energy harvesting system provides a powerful application, for use within the particular areas, in order to avoid the maintenance processes accessing with human or be manned remotely for manipulating the wireless device operations, yet the vibration energy should be available continuously or discretely for transferring the ambient waste energy into this harvesting system. Even though the transmitter device is located very far from the receiver (i.e. peripheral wireless devices and its server receiver), the electrical energy storage proposed in this dissertation definitely confirms that the vibration energy harvesting using piezoelectric generators undergone the discrete harvesting system is significantly feasible for application in real practical operations as a transmitter/receiver sensor node upon the stand-alone system.

CHAPTER 1

INTRODUCTION

The pre-introductory chapter is to introduce the definition of two terms which is the main idea of the thesis within these particular issues: ***Piezoelectric Material*** *and* ***Energy Harvesting****.* ***Piezoelectric Material*** *is a material that has the ability from its crystalline property to transform mechanical energy into the electricity, and vice versa, to convert an applied electrical potential into a mechanical strain on its matter (Sodano et al., 2004). Consequently,* ***Energy Harvesting*** *process is started when the material is bonded on the specific structure that is able to capture and harvest the ambient energy from the environment (i.e. sunlight, temperature, radio frequency, and vibration) (Caliò et al., 2014).*

1. Introduction

In this last decade, the embedded system, microcontroller or microprocessor combined with many functional workings: timer/counter, A/D (analogue to digital converter), D/A (digital to analogue converter), register bank, memory, etc., was an extremely sophisticated technology to drive modern innovations. People used them, but they did not know what was inside. Based on the definition of the embedded system design (Vahid and Gevargis, 2002), IoT (Internet of Things), defined in one kind of many groups of microcontrollers, was a multifunctional microcontroller. Even though, in that period of time, the principle definition of IoT technology was a promising technology in the near future.

Nowadays, a modern technology based on IoT (i.e. Arduino, Raspberry Pi, Node-MCU, ESP32, PM-2.5 sensor, temperature, and humidity sensor) has emerged from specific group researchers or users. It is known as open-source software and hardware. In terms of the IoT system, the wireless sensor node (WSN) is implemented in this system as well as being connected as a network for working together. However, the devices obviously need electrical power for their functions. In addition, the power

consumption would be increased more by the peripheral sensor. As a common idea, a battery is a very simple and realistic power source for these devices, but the environmental and economic issues could not be addressed as easily for managing as proper processes of electronic hazardous wastes (Lallart et al., 2008). Therefore, the way of this solution is to find a new type of the energy source by using the Vibration Energy Harvesting Using Piezoelectric Method.

This study aimed to investigate the standalone power generator in order to research the potential of the smart environmental management using a conventional piezoelectric material for supplying the electricity to a battery-less device. The validation is focusing upon discrete vibrations from an air-compressor outdoor unit as a vibration source. Furthermore, this system has used a basic circuit, which is a bridge rectifier, to transform an Alternating Current (AC) into a Direct Current (DC) for driving a wireless receiver without an additional enhancement circuit. The research deliverables are implemented by the recent dramatic increase of IoT technology in a practical area where there are ultra-low acceleration and magnitude of vibration. Moreover, its applications are able to be demonstrated in simple environmental parameters using a wireless transmitter which is able to send data from connected peripheral sensors. The wireless receiver then receives this data by using the simple piezo-power generator from the vibrating air-compressor unit.

The introductory chapter provides the thesis overview regarding research motivations and statements of these problems. These following topics are summarized within three relevant subjects. The first subject is the **Motivation and Statements of the Piezoelectric Method**. In this part, the research motivation declares its problems as problem-based research under a discontinuous and very low power on energy sources of a piezoelectric material in global-area usage. Then, these problems are able to be investigated by using the local environment or devices, such as using an air-compressor unit at Prince of Songkla University (PSU) in Thailand or around the local area. In addition to the first topic on research motivation, another subtopic is the **Statements of the Technology** where they are the piezoelectric materials and the related techniques necessary regarding this subject. Before the latter, **Organization of the Thesis**, many chapters of the thesis are presented in this subject, this is the entire work outline as well

as representing in each a different main purpose. Every chapter describes its research scope for backing up the research objectives. Finally, the **objectives of the research** are, therefore, to be a summary part of this research.

1.1. Motivations and Statements of The Piezoelectric Method

1.1.1. Motivations of The Research

The Vibration Energy Harvesting (VEH) using Piezoelectric Method will be the key point of this research goal which focuses on its possible applications and realistic implementation in the case of a conventional air-compressor outdoor unit. Its implementation is influenced by current situations of using wireless technology and environmental problems as well as potentially practical implementations of the piezoelectric energy harvesting method. Thus, it will be briefly explained why the motivation occurs, and this project then is launched in this situation.

The piezoelectric energy harvesting method, the number of electronic products in the market trying to apply an energy source from the ambient environment and/or human movement; the Enocean (www.enocean.com) product is completely accomplished by using a small solar panel and an electromagnetic switch. But the piezoelectric method of another footwear product, it appears to be implementing this piezoelectric patch thus applying a piezo-material as a sensor not to produce power (Anderson, 2011). In this case, it was implied that this piezo-material has its capabilities to be a power generator due to its signal caused by the footstep, and the electrical power could be accumulated because the signal intensity can be detected clearly. Following this reason, this research objectives would likely validate the necessary parameters for their new implementation on air-compressor units to assign this piezoelectric material being a power source from vibration. Hence, it would be possible to capture the electrical power from a continuous and discontinuous vibration system then storing the electrical current into capacitors.

In addition to the piezoelectric energy harvesting method, there is another reason for choosing the air-compressor as a vibration source owing to

environmental issues (Krikke, 2005). According to a report by the International Energy Agency (IEA, 2018), worldwide air-conditioners are predicted to be rapidly increasing in around the world from 1.6 billion units today in 2016 to 5.6 billion units by midcentury in 2050. Unfortunately, greenhouse gas emissions are also released by coal and natural gas plants while they are generating the electricity to power those air-conditioners. The power plants would nearly expose double greenhouse gas, from 1.25 billion tons to 2.28 billion tons in the same period, as shown in Figure 1. Therefore, those emissions would contribute to the global warming which could dramatically heighten the demand for air-compressor units. Finally, not only the number of air-compressors around the world but also the mechanical vibrations of their compressor units have influenced the selection of them as a free and available vibration source for this system of the vibration energy harvesting.

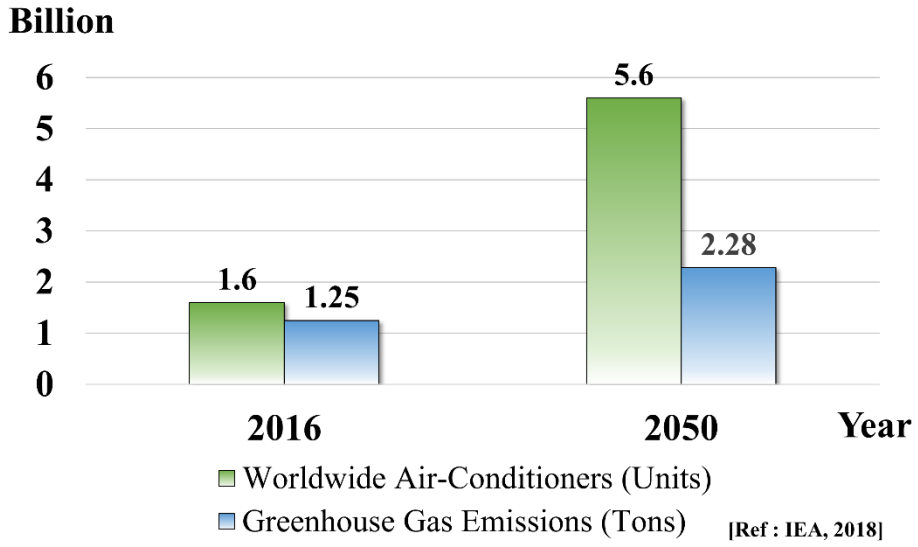

Figure 1.1 The number of air-conditioners increasing in the world with greenhouse gas emission effect.

1.1.2. Statement of The Piezoelectric Method

The purpose of this section is to review piezoelectric energy harvesting method that is especially related to the vibration harvesting technique, such as energy harvesting technology, piezoelectric material principle, electromechanical modelling of piezoelectric material, interfacing circuit, and possible applications. These topics

represent the state of the art in piezoelectric energy harvesting on vibration using a smart material method within the last decade.

1.1.2.1. Energy Harvesting Technology

In this topic, energy harvesting technology is an overview concept of energy harvesting techniques with many application areas on each type of energy harvesters. The principle and type of output powers would also be shown their relation in this diagram.

Figure 1.2 would be defined as a classified diagram of the main energy harvesting technologies in which the hierarchy could be divided into 2 branches. Starting from the top level for this research, **Energy Harvesting** is especially focusing on an ultra-low-electrical power of output power generators by following various ambient sources. Then, the next level is specified by mainly regarding the **Application Field** and **Working Principle**; these two blocks are also linked to the **DC Output** and **AC Output** power of harvesters and these last two dash-blocks contain various principles of many energy-harvesting types, e.g. solar, thermal, RF, and motion. Finally, the corresponding applications, which relate to its effect or method of energy conversion, are to be presented by using this diagram throughout these issues of the application for **Motion movement** and the **Piezoelectric** material implementation.

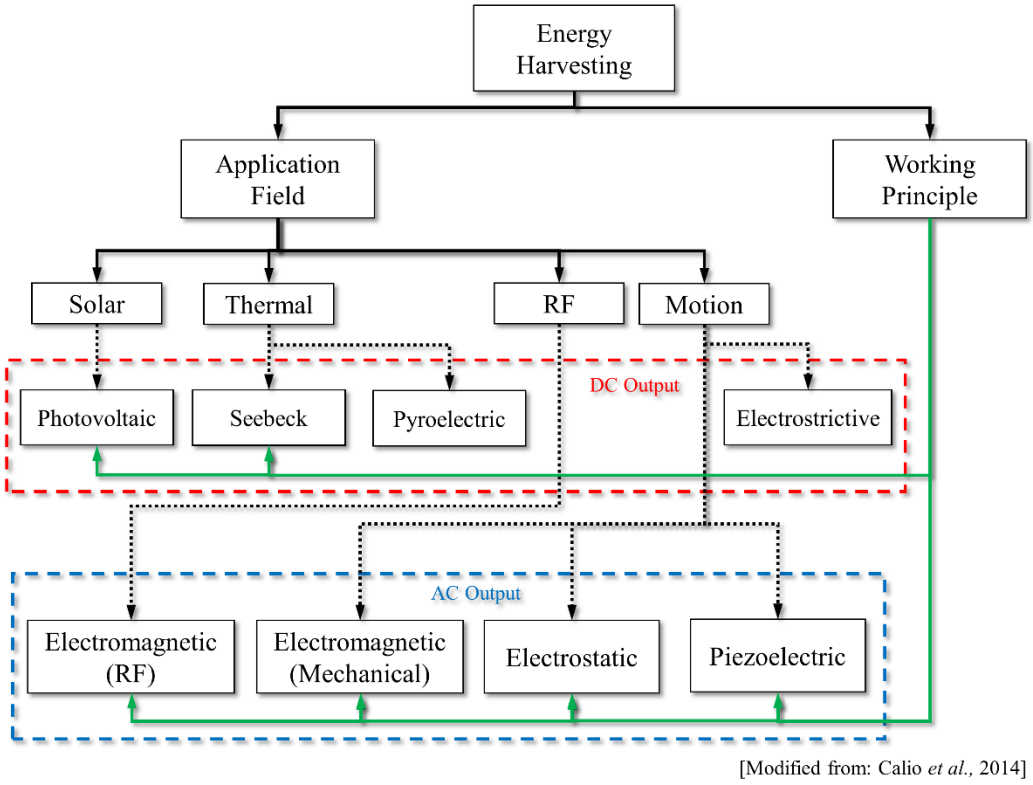

Figure 1.2 Diagram of energy harvesting technologies.

The main dedication in this diagram only focuses on fundamental concepts of the piezoelectric vibrating structures despite the basic of vibration-into-electricity (**Motion**) as a consequence of the material effect (**Piezoelectric**). The mechanisms of energy conversion are able to be divided into three types; **electromagnetic(mechanical)**, **electrostatic**, and **piezoelectric** (Dicken et al., 2012; Arnold, 2007; Torah et al., 2008; Jung et al., 2015; Sodano et al., 2005; Williams and Yates, 1996; Roundy et al., 2003; Roundy et al., 2002; Roundy and Wright, 2004). Thus, its constitutive behaviour of the piezoelectric method as well as including the standard circuit interface could be expressed as a valid model review within the next following section.

Moreover, the most promising technologies based on micro-scale energy harvesting extracted energy from vibration, different temperature, light, and RF emissions appear to be clear of interest nowadays, but the available energy is obviously lower than consuming possibilities to electronics devices as sufficiently as possible.

The approximate amount of energy per unit is available thus following the micro-scale of harvesting sources, as given Table 1.1.

Table 1.1 Estimation of the power density from the different-source energy harvesting (Raju and Grazier, 2010).

Energy Source	Harvested Power
Vibration/Motion	
Human	4 μW/cm^2
Industry	100 μW/cm^2
Temperature difference	
Human	25 μW/cm^2
Industry	1 - 10 mW/cm^2
Light	
Indoor	10 μW/cm^2
Outdoor	10 mW/cm^2
RF	
GSM	0.1 μW/cm^2
WiFi	0.001 μW/cm^2

1.1.2.2. IoT Based-on Its Vibration Energy Harvesting Concept

According to the previous section, environmental pollution has been the main problem to challenge the researchers due to the effects on mankind. Piezoelectric materials can be used as a means of transforming surrounding vibrations into electrical energy to power devices. The focus is on an alternative approach to scavenge energy from the environment. Therefore, it is the reason in which vibration energy harvesting is provided.

The IoT issue as an interesting and promising technology, by the near future in the year 2020, there would be 50 billion of smart μ-computers around the living area of the human being (Evans, 2018). In this foresight of the *smart environments* with including the *pervasive computing*, many miniature computing devices would be integrated into every object and daily activities, and the people could be empowered to be the better for *human-nature computing cooperation* (Tan, 2013).

As also being the mentioned research to accomplish this goal could be the solution consisting of two main perspectives. **The first** solution is to design the

harvesting structure for the specific task. Then, **the second** is to manage the electrical power for proper devices. In general equipment with sensing, processing, and communicating functions, are also known as a Wireless Sensor Device or Node (WSD). When these WSDs are connected, they form their own network or shared with others. It is called the Wireless Sensor Network (WSN).

In conclusion, this research, therefore, focuses on the piezoelectric material to be a transducer for vibration energy harvesting. The battery-less device, bridge rectifier and stand-alone wireless sensor device are also particularly investigated in this research.

1.2. Organization of The Thesis

This dissertation consists of five chapters. In this chapter is presented the background and statement of the piezoelectric energy harvesting.

Then, Chapter 2 illustrates the theory of a vibrating structure focusing on energy harvesting cantilever thus following an introduction to a vibration energy harvesting using the piezoelectric method based on the direct current (DC) circuit for battery-less implementation.

Furthermore, Chapter 3 is to describe and analyze the research methodology of this dissertation as well as the experimental design also presented.

The following section before the last chapter, Chapter 4, would be the results and discussions which are related to the previous chapter.

Conclusions and suggestions for the further work are given in Chapter 5 which is the final chapter.

1.3. Objectives of Research

The objective of this research is to investigate the electrical power from the vibration using the piezoelectric transducer as energy conversion. By using a conventional source for vibration, an air-compressor outdoor unit selected in order to

be a discrete vibrating excitation. Three strategies of this investigation have been determined by the particular regarding:

1. To propose the electromechanical modelling based on a piezoelectric material method by using the stress and electric field relations of piezoelectric equations in terms of the DC power model.
2. To adapt the energy harvester for the vibration using a piezoelectric material on a cantilever (beam) structure under the low vibrating acceleration thus putting this structure on an air-compressor unit.
3. To provide an interfacing part between the air-compressor unit and a storage capacitor.
4. To manipulate an electrical output into applications for environmental management implementations.

CHAPTER 2

PIEZOELECTRIC ENERGY HARVESTING

This chapter had an explanation of a twofold reason, in which these particular problems would be presented the Forced Harmonic Vibration (Thomson, 1993; French, 1971; Inman, 2014) and Base Excitation Vibration (Inman, 2014; Thomson, 1993; Kelly, 2012). Moreover, the principle appears to be proposed as a simplified model and presented by developing the strain-charge expression of the piezoelectric electromechanical modelling based on a lump diagram regarding to a DC power using a standard circuit (conventional bridge-rectifier).

2. Piezoelectric Energy Harvesting

The principle of electromechanical of vibration energy harvesting using the piezoelectric method is presented in this chapter. This modelling, that is regarding the research experiments, is probably contributed to such following contents: fundamental of the piezoelectric effect, vibration and energy harvesting, and electromechanical energy harvesting.

2.1. Fundamental of Piezoelectric Effect

This paragraph presents a brief introduction of the piezoelectric material followed by the related expressions and parameters. Before the reveal of a piezoelectric effect, in 1880, the piezoelectric effect was discovered by the brothers, Jacques Curie (1856–1941) and Pierre Curie (1859–1906), with their studies of conclusive surface charges appearing on special prepared crystal from crystalline mineral, e.g. Rochelle salt, tourmaline, cane sugar, topaz, and quartz. It showed that the generated voltages of the opposite polarity and proportional to applied loads were induced by the tension and compression thus defining as the *direct effect*. The year before the end of 1881, the Curies brothers also confirmed their experimental results in the existing of another

effect. They showed that the lengthened or shortened deformation of the crystal was exposed by an electric field corresponding to the polarity of the field and proportional to the field strength. It was called the *inverse effect* (Dineva et al., 2014). The overview of these two effects are shown in Figure 2.1

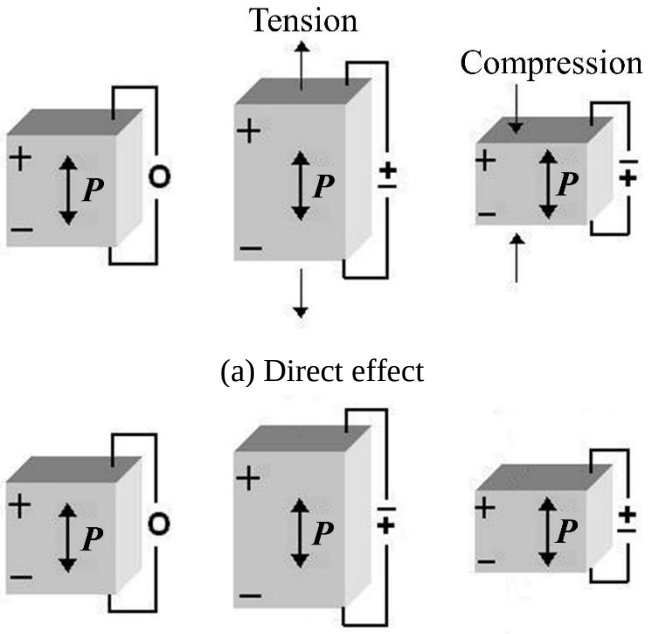

(a) Direct effect

(b) Inverse effect

Figure 2.1 Piezoelectric effects (Source: https://www.bostonpiezooptics.com/intro-to-transducer-crystals).

Nowadays, the piezoelectric materials have developed their material properties, compositions, and shapes, as well as used in many devices to be a transducer and an actuator, such as ultrasound microphones and speakers, ultrasonic imaging, and hydrophones. In another approach of piezoelectric applications within two decades after the widespread technology of WSN, these applications are used as a power generator from the scavenging ambient energy in the case of vibration, that is captured by the proper designed structure.

The two basic structures will be considered throughout their material properties. The piezoelectric charge coefficient is defined as the dielectric displacement, which is governed per unit of an applied stress, under a constant electric

field. So, it has a unit of C/N. The piezoelectric materials show their properties of the anisotropic crystal axis (Figure 2.2 (a)); the *d* coefficients are generally indexed by two subscripts that indicate the directions of the two related quantities. Therefore, the *d* coefficients with respect to the two modes of the generator are designed as the longitudinal (d_{33}) and transverse (d_{31}) piezoelectric coefficients, Figure 2.2(b) and Figure 2.2(c) respectively. The *d31* coefficient is the generated electric polarization along the *z*-direction per unit of applied stress in the *x*-direction, while the *d33* coefficient describes the produced electric polarization along the *z*-direction per the unit of applied stress in the same direction.

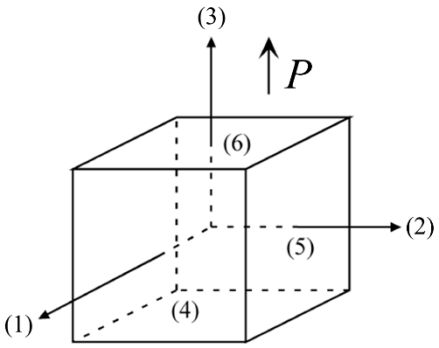

(a) Axes notation.

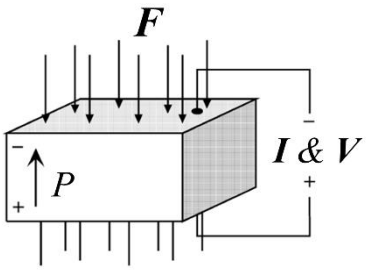

(b) Compression Generator (33 mode).

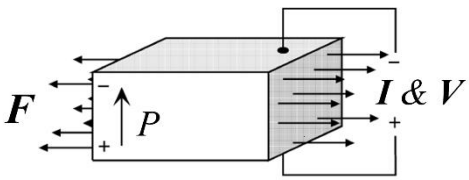

(c) Tension Generator (31 mode).

Figure 2.2 Mode of the piezoelectric generator under axes notations (a) within 33 mode (b) and 31 mode (c) (Source: (González et al., 2002)).

Taking into account of VEH devices applying to practical applications, their constitutive expressions of piezoelectric materials could be illustrated by the relationship of the strain-charge forms, as shown in (2.1) and (2.2):

$$S = s^E T + dE \ , \tag{2.1}$$

$$D = dT + \varepsilon^T E \ . \tag{2.2}$$

The first equation, corresponding to the direct effect could be defined by the mechanical strain *S* undergone by two terms of mechanical and electrical characteristics. The mechanical property is led to the elastic compliance s^E measured under a short circuit condition multiplied by the mechanical stress *T*. Another term is the electrical property consisting of the piezoelectric constant *d* with the electric field *E*. The latter expression has exposed the electric displacement or charge density *D* representing the inverse effect. The mechanical property is linked to the piezoelectric constant with the mechanical stress. In addition to the mechanical property, the electrical property is also combined the material permittivity of the dielectric property as measured by a free clamped condition ε^T with across the electric field.

2.2. Modelling of Piezoelectric Energy Harvesting

The electromechanical principles with a cantilever beam structure bonded the piezoelectric material for capturing energy from ambient vibration will be presented in two methods of applied force positions in the same structure. The first one is a direct force that is applied at the free-end side on this beam (Figure 2.3. (a)) (Guyomar et al., 2005; Rakbamrung et al., 2010). The second one is an indirect force that is applied to a position of the base structure (Figure 2.3. (b)) (Lefeuvre et al., 2007; Dicken et al., 2012).

This section briefly presents an overview of the piezo-electromechanical model, which is developed from the electromechanical principles. This main purpose is to show the related model parameter of two configurations; the basic concept of direct

force before developing, and the further configuration of the indirect force. Moreover, the designed structure is very considerable, so the following development is to be exhibited the output power of their approaches. These are two cases that will be considered:

- The case I – *harvester behaviour*, the force that drives the system at the resonance frequency of the beam leads to the significant displacement and acceleration.
- The case II – *energy harvesting technique*, the majority of the enhanced energy with the simple circuit technique, bridge rectifier circuit or a standard technique, that can be harvested within the range of resonance frequency bands.

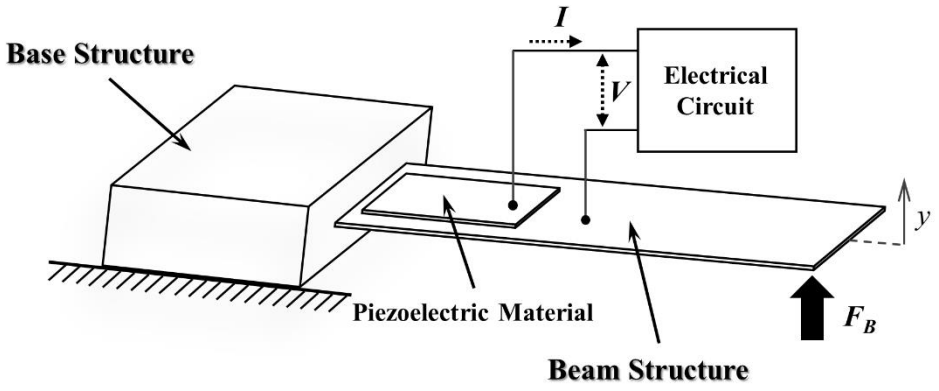

(a)

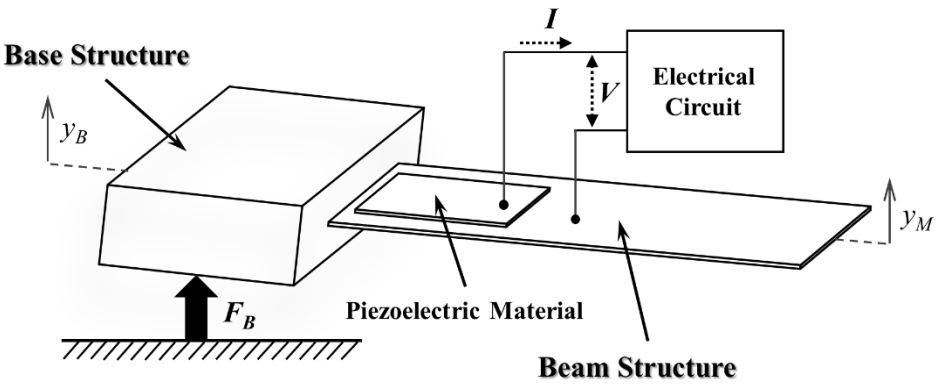

(b)

Figure 2.3 Schematic drawing of the experimental set-up regarding two-type differences applied input force (F, F_B) to a direct force (force motion) (a) and an indirect force configuration (support motion) (b).

2.2.1. Piezo-Electromechanical and Direct-Force Principle

The piezo-electromechanical model including with the harvesting vibration structure occurred by adding the piezoelectric element can be described as in a single-degree-of-freedom (SDOF) diagram. This schematic structure composes the main functional components related to the differential equation of this system. The first component is the system motion mass *M*. The second component is the spring K_S corresponding to the stiffness of this structure. The third component is the dashpot *C* purposing to dissipate energy and to damp the response of a mechanical system. The latter one is the piezoelectric element which is to convert mechanical energy to electrical energy undergone by the harvested beam structure (Figure 2.4 (a)).

This harvester is excited around its first resonance frequency ω_0. Also, this system responds easily at low frequency due to the high acceleration magnitude (Roundy, Wright, and Rabaey, 2003). The driven force *F*, Equation (2.3) (French, 1971), as a function of an input angular frequency ω induces the mass displacement *y*, Equation (2.4) (French, 1971), following Newton's law, as shown in Figure 2.4 (b).

$$F = F_B = F_0 \cos(\omega t). \tag{2.3}$$

$$y = Y_0 \cos(\omega t - \delta_1). \tag{2.4}$$

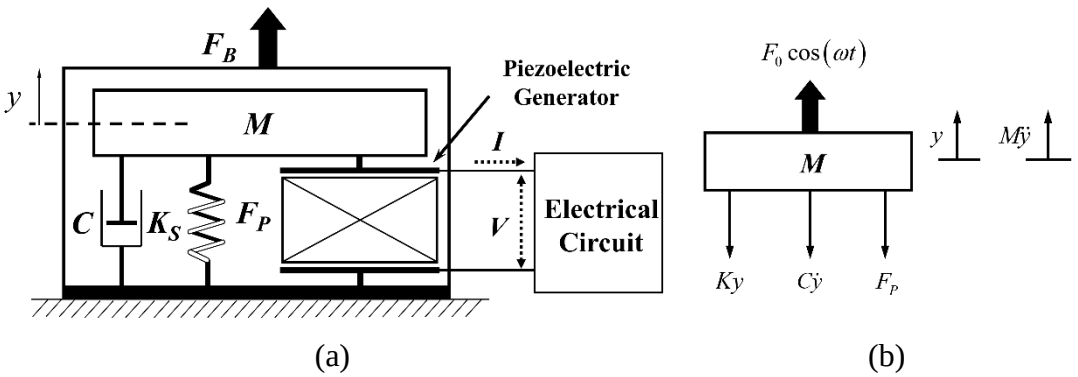

(a) (b)

Figure 2.4. Direct-force configuration, schematic including the piezoelectric material generated the electrical power (a), the free-body diagram to analyze model parameters (b).

According to the IEEE standards relating to piezoelectricity, the piezoelectric equations can be written as,

$$\begin{cases} T = c^E S - eE \\ D = eS + \varepsilon^S E \end{cases}, \tag{2.5}$$

where ε^S is the dielectric permittivity at a constant strain, c^E is the elastic stiffness in a short circuit condition, and e is the piezoelectric coefficient of the materials.

The piezoelectric generator equations (2.5) can be linked to the mechanical variables (y, F_P). The electrical variables (I, V) can be rewritten into the consideration motion as given (Roundy, Wright, & Pister, 2002),

$$\begin{cases} F_P = K_P^E y + \alpha V \\ I = \alpha \dot{y} - C_P \dot{V} \end{cases}, \tag{2.6}$$

where F_P is the piezoelectric restored force, and I is the piezoelectric current. These two variables are under y, which is the vibration direction. C_P is the material capacitance related to the α, which is the applied force (Guyomar et al., 2009), and K_P^E is the short-circuit stiffness of the piezo-element.

Therefore, the equivalent lumped model for a monomodal structure is given by a simple spring-mass-damper system with a piezo-electromechanical coupling described by Equation (2.7) (Rakbamrung et al., 2010). The open-circuit condition due to the piezoelectric voltage is vibrated with uncontrolled conditions. The sum of K_S and K_P^E is signified as the global stiffness K of the harvester.

$$\begin{cases} F = M\ddot{y} + C\dot{y} + Ky + \alpha V \\ I = \alpha \dot{y} + C_P \dot{V} \end{cases}. \tag{2.7}$$

Electrical power P_{DF} is produced by the piezoelectric generator through sinusoidal excitation, which is a steady-state operation (Guyomar et al., 2009). This

circuit interfacing is the so-called Standard Circuit which is connected as following this Figure (2.5).

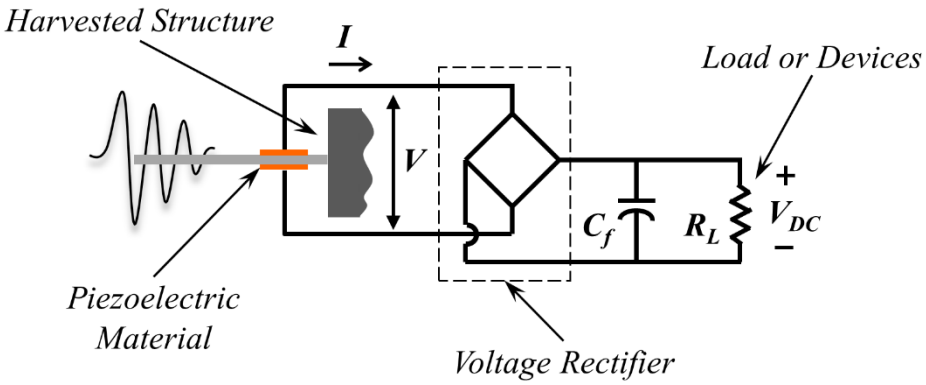

Figure 2.5 Bridge rectifier interface.

The displacement of the structure at the operation frequency ω_0 is the constant magnitude, F_M. The power output from the piezoelectric generator is related to the load resistance, R_L. Therefore, the power output equation is given below (2.8).

$$P_{DF} = \frac{R_L \alpha^2}{\left((\pi/2) + R_L C_P \omega_0\right)^2} \frac{F_M^2}{C^2} \ . \tag{2.8}$$

In the case of harvesting power by the load resistance, its harvesting power is able to reach as the maximum point at the optimal value of resistance R_{opt} (Guyomar et al., 2005; Lefeuvre et al., 2006), yielding Equation (2.9). With respect to the optimal resistance at the value R_{opt}, the ideal maximum power $P_{DF\text{-}MAX}$ can be expressed by Equation (2.10).

$$R_{opt} = \frac{\pi}{2\omega_0 C_P} \ . \tag{2.9}$$

$$P_{DF-MAX} = \frac{\alpha^2}{2\pi C_0 \omega} \frac{F_M^2}{C^2} \ . \tag{2.10}$$

2.2.2. Indirect-Force Principle Development

The provided principle in this sub-section is aimed to see a basic manner of a Vibration-Energy-Harvesting cantilever on seismic structures and a perception of circuits interface. The electricity is harvested from vibration energy thus consuming the electrical power to the low-power electronic devices. The discrete ambient force is initiated from the discontinuous operating of base-excitation systems (i.e. air compressor, air pump, washing machine). The mechanical energy from these systems has to be transferred to the cantilever with the piezoelectric specimen moving to the storage device at the optimal point. Hence, the analysis of the harvester coupled with the electrical circuit will be undertaken.

As the lumped model mentioned in the previous section, the motion of the mass is related to the base of the seismic structure which is denoted by $y = y_M - y_B$.

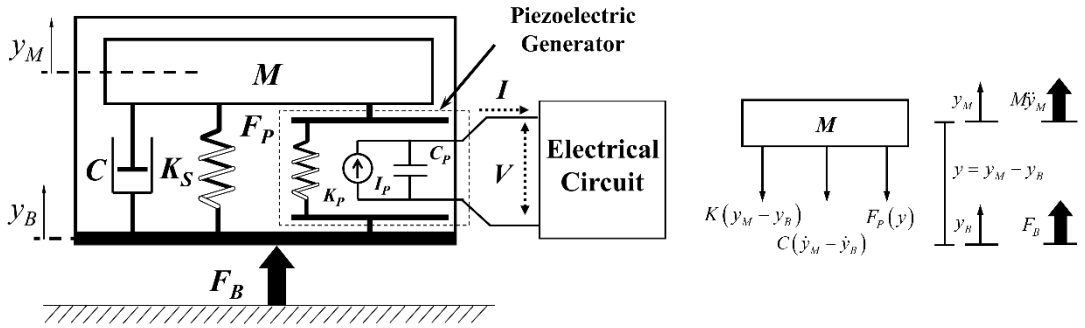

(a) (b)

Figure 2.6 Indirect-force configuration, the schematic (a) and free-body diagram (b).

The modelling diagram was developed by the direct-force principle (Richard, Guyomar, and Audigier, 1999; Richard, Guyomar, Audigier, et al., 1999; Guyomar et al., 2005) which is represented in Figure 2.6 (a). The balance of forces on this system referred to Figure 2.6 (b). As a result, the diagram description of the force is defined thus being the piezo-electromechanical on the indirect-force configuration (base excitation or base motion method), and the electrical model is integrated into the

electrical schematic of the mechanical model as a part of the piezoelectric material replacing, which is developed from Ottman *et al.* and Lefeuvre *et al.* (Ottman et al., 2003; Ottman et al., 2002; Lefeuvre et al., 2007), by yielding on Equation (2.11)

$$M\ddot{y}_M + C\left(\dot{y}_M - \dot{y}_B\right) + K_S\left(y_M - y_B\right) = F_B - F_P \ . \tag{2.11}$$

The vibration energy harvesting using piezoelectric effect can also be explained by equations (2.12). These relations due to piezoelectric constant *d* will be presented with regard to a simple beam structure corresponded to the material mode of the piezoelectric generator within 31 mode (Erturk and Inman, 2008). Equation (2.13) is related to the stress *T* and electric field *E* (Ikeda, 1990).

$$\begin{cases} S = s^E T + d_{31} E \\ D = d_{31} T + \varepsilon^T E \end{cases} . \tag{2.12}$$

Expressions (2.12) lead to relations that become these expressions (2.13). The piezoelectric restoring force F_P and displacement *y* can be defined as these mechanical variables (F_P, *y*). The flowed current *I* through the load resistance as an electrical circuit or devices, and the piezoelectric voltage *V* across parallel with both side electrode can also be defined as these electrical variables (*I*, *V*).

$$\begin{cases} F_P = K_P^E\left(y_M - y_B\right) - \varphi V \\ I = d_{31}\dot{F} + C_P\dot{V} \end{cases} . \tag{2.13}$$

Equations (2.14), (2.15), and (2.16), in these two terms of F_P and *I* expressions are given, the restoring piezoelectric force of the piezoelectric voltage coefficient φ, the short-circuit stiffness K_P^E of the piezoelectric element, and the piezoelectric-disk capacitance C_P clamped on spring-steel beam, the electrode area on the piezoelectric-disk a_e and the thickness of the material t_0.

$$\varphi = \frac{d_{31} a_e}{s_{11}^E t_0} \ , \tag{2.14}$$

$$K_P^E = \frac{a_e}{s_{11}^E t_0} \ , \tag{2.15}$$

$$C_P = \frac{\varepsilon_{33}^T a_e}{t_0} \ . \tag{2.16}$$

Where d_{31}, s_{11}^E and ε_{33}^T are the representative of the piezoelectric coefficient, the elastic compliance at the constant electric field, and the dielectric permittivity at the constant mechanical stress, respectively.

The following parameters are corresponded to the energy ratio, the global coupling factor *k* thus representing as the definition of the conversion between electrical to mechanical energy or vice versa. The global coupling factor is defined by Mason (Mason, 1935), yielding (2.17):

$$k^2 = \frac{stored\ \ mechanical\ \ energy}{supplied\ \ electrical\ \ energy} \ , \tag{2.17}$$

the piezoelectric coupling factor k_{31} derived from the definition (2.17) can be expressed as the following Equation (2.18) (Ikeda, 1990),

$$k_{31}^2 = \frac{d_{31}^2}{\varepsilon_{33}^T s_{11}^E} \ . \tag{2.18}$$

In the short circuit condition, the mechanical variables are substituted into Equation (2.11) due to the mechanical property under the free vibration regarding a steady-state oscillation. The equation can be rewritten as the following expression (2.19).

$$M\ddot{y} + C\dot{y} + \left(K_S - K_P^E\right) y = F_B \ . \tag{2.19}$$

For another case, the open circuit condition due to the piezoelectric voltage with respect to electrical variables is linked to the dynamic equation at steady-state vibrations undergone by the applied restoring force, and the K_S and K_P^E signified as the global stiffness *K* of the harvester are summed by the condition of the harvesting structure and transducer corresponded by the vibrating structures. The equation (2.13) can be substituted into Equation (2.11) as coupled relations of the piezoelectric generator due to the uncontrolled condition. Therefore, the coupled piezo-electromechanical expression based on the indirect-force configuration can be written as (2.20):

$$\begin{cases} -M\ddot{y}_B = M\ddot{y} + C\dot{y} + Ky + \varphi V \\ I = d_{31}\dot{F} + C_P\dot{V} \end{cases} . \tag{2.20}$$

Before accessing the section of energetic analysis, the governing motion expression of the mechanical term in the previous Equation (2.20) can be determined by the mechanical parameters of this structure on a free-vibration condition by using this differential equation (2.21),

$$\ddot{y} + \gamma\dot{y} + \omega_0 y = 0 . \tag{2.21}$$

The mechanical quality factor *Q* (2.22) can be defined by the damped oscillation characteristic of these two quantities: the damping factor γ (2.23) and natural angular frequency ω_0 (2.24). The constant vibration magnitude at the angular frequency ω_0 is corresponded by controlled conditions with regard to undamped oscillations, and the damping factor γ is a reciprocal identification of the time required for the energy decrease belonging to the characteristic of damped oscillations. Nevertheless, the damping ratio ζ (2.25), when $0 < \zeta < 1$, is also a mutual relation with the damping coefficient *C* due to the case on the *underdamped* motion condition.

$$Q = \frac{\omega_0}{\gamma} = \frac{\sqrt{KM}}{C} , \tag{2.22}$$

$$\gamma = \frac{C}{M} \ , \tag{2.23}$$

$$\omega_0 = \sqrt{\frac{K}{M}} \ , \tag{2.24}$$

$$\zeta = \frac{C}{2\omega_0 M} = \frac{1}{2Q} \ . \tag{2.25}$$

According to expressions (2.20) referred to such mechanical variables that are defined by the dynamic balance of the forces governing the displacement of the mass. The equation of the mechanical energy (2.26) is obtained by multiplying both terms of the mechanical variable equation with the velocity and integrating over the time variable. The provided energy, that is rewritten by the mass term related to the angular input frequency with a displacement of the base structure, is divided into kinetic energy, elastic potential energy, mechanical losses, and transfer energy from the harvesting structure.

Another Equation (2.27) is substituted to such the expression of electrical variables by multiplying the electrical voltage as well as using the same previous processes. The left term of the expression will show the relations of absorbed energy by connected electronic devices. Another right term of the expression of the electrical power absorption, that is the two terms of the piezoelectric voltage and current, is consisted of the transferred energy from piezoelectric materials as a function of the applied force over the electrode area and the stored electrostatic energy by the piezoelectric disk capacitance.

$$\int M\omega^2 y_B \dot{y} dt = \frac{1}{2} M\dot{y}^2 + \frac{1}{2} Ky^2 + \int C\dot{y}^2 dt + \int \varphi V\dot{y} dt \ , \tag{2.26}$$

$$\int VIdt = \int d_{31} V\dot{F} dt + \frac{1}{2} C_P V^2 \ . \tag{2.27}$$

Finally, regarding the beam structure with the piezoelectric element located on the base sinusoidally oscillating, the alternating current and voltage will be

driven from the piezoelectric specimen. The generated signals are necessary to convert to DC. This piezoelectric disk was connected to a standard-circuit interface consisting of a diode bridge rectifier, filtering capacitance (smooth voltage/current) and the resistance load R_L (Figure 2.5). Thus, the harvested power P_{IDF} vibrated at the resonance frequency f_0 as a function of the load resistance can be determined by using the following equations:

$$P_{IDF} = \frac{V_{DC}^2}{R_L} = \frac{\left(4d_{31} f_0\right)^2 R_L}{\left(1+4C_P R_L f_0\right)^2} F_0^2 \ . \tag{2.28}$$

In the case of harvesting power, it is able to reach a maximum point at the optimal resistance $R_{opt\text{-}IDF}$ (2.29), where ω_0 is a natural angular frequency at a resonance frequency. When the resistance R_L is being approached to be a maximum value thus reaching the optimal resistance value $R_{opt\text{-}IDF}$ (2.29), the maximum power of the indirect force method $P_{IDF\text{-}MAX}$ can be yielded as given in expression (2.30),

$$R_{opt-IDF} = \frac{1}{\omega_0 C_P} \ , \tag{2.29}$$

$$P_{IDF-MAX} = \frac{16\left(d_{31} f_0\right)^2}{\left(1+\frac{4 f_0}{\omega_0}\right)^2} \cdot \frac{F_0^2}{\omega_0 C_P} \ . \tag{2.30}$$

2.2.3. Piezoelectric Harvester Equivalent Circuit Model

The equivalent circuit model for piezoelectric material (ceramic or polymer) can be defined by the latest diagram of the electromechanical model, Figure 2.6. The model presents its components with a relation of the piezoelectric generator behaviour between the mechanical structure and the electrical circuit transformation.

Figure 2.7 illustrates the electrical view parameters linked to the flowed current I (2.20). In the open-circuit condition at the steady-state vibration, the flowed current from piezoelectric transducer I_P is undergone by two terms of mechanical aspects and electrical properties. The mechanical aspects are composed of the material properties, in which the restoring force across the material electrode $\dot{F}$ corresponded to the scavenging structure as a function of the base-structure with the material stiffness K_P is multiplied by the piezoelectric coefficient d_{31}. Moreover, another added term of the material characteristic is the electrical properties, where the piezoelectric patch corresponds to the material capacitance C_P as a function of the open-circuit voltage upon the scavenging structure $\dot{V}$.

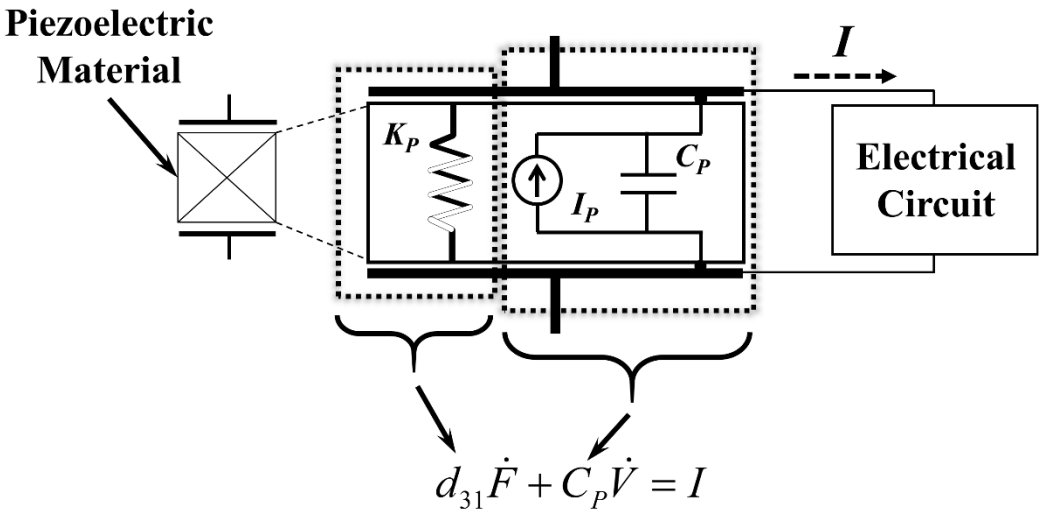

Figure 2.7 Equivalent circuit of the piezoelectric material (electrical view).

Hence, Due to the output from material throughout connected devices, the piezoelectric voltage as a DC output is transformed by the similar AC signal with an internal resistance; for instance, in terms of the DC-component resistance term after the bridge rectifier circuit included the internal complex and non-complex resistance of the piezoelectric materials, and the filter capacitor is to be assigned as an internal resistance of the piezoelectric generator.

According to the equivalent circuit, as proposed by Figure 2.7, the DC voltage could be assigned by this expression (2.31),

$$V_{DC} = \frac{4d_{31} f_0 R_L}{1 + 4C_P R_L f_0} \cdot F_0 \ . \tag{2.31}$$

In which this equation, V_{DC} is a rectified output from a conventional full-wave rectifier circuit as a function of the applied force F_0 related to the area of the material electrode. The optimum resistance of the piezoelectric generator is R_L with respect to the resonance frequency f_0 of the harvested structure including material parameters, where they are illustrated by the piezoelectric capacitance C_P and piezoelectric material coefficient d_{31}.

2.3. Power Optimization Technique

Based on the model presented in the previous section, the power of a piezoelectric generator is strongly dependent on the load resistance. The power is at a maximum for one or two matching optimum loads. The FoM (Figure of Merit), as given expression (2.32), needs to be greater than 2 in order to charge a rechargeable battery (Sodano, Park, Leo, & Inman, 2005). The values are determined by the piezoelectric generator based on its electromechanical characteristics and depending on the particular vibration frequency of the ambient excitation source (Guyomar et al., 2005; Rakbamrung et al., 2010).

$$k_t^2 Q_{str} \ , \tag{2.32}$$

Where FoM is expressed as the electromechanical coupling factor k_t^2 corresponded of the material's conversion property and the structural quality factor Q_{str} linked the harvested structure property corresponded to the structural vibration capturing the available mechanical energy.

The piezoelectric generator is a simple cantilever beam formed from the piezoelectric material. The beam structure can capture ambient vibration sources based on their resonance frequencies, and the operating frequency is defined at around the near resonance. Therefore, the beam structure is able to produce the maximum power output and a DC output can be obtained using a rectifier circuit, as shown in Figure 2.7.

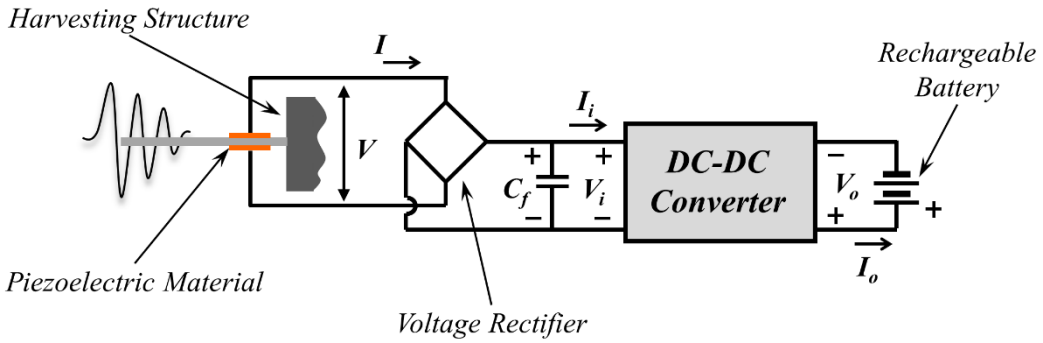

Figure 2.8 Schematic of the circuit interface for charging rechargeable batteries using piezoelectric materials as power generators.

Generally, the maximum electrical power from the single piezoelectric generator is unable to charge a rechargeable battery, even when the piezoelectric voltage is higher than the battery voltage (Hart, 2011; Thainiramit, 2013). To solve this problem, a buck-boost circuit is applied. This dissertation presents the output power P_{DF} (2.8) of an experimental investigation by employing the output power from the piezoelectric material throughout the Continuous Current Mode (CCM), and the relevant parameters of the Discontinuous Current Mode (DCM) can be derived from the CCM. The CCM can be implemented in the piezo-electric parameters based on the electrical threshold condition with both minimum current and inductor size as well as load resistance related to the output power.

2.3.1. Switching Technique for Harvesting Circuit

The schematic of the buck-boost circuit presented in Figure 2.8 is only the simple components that follow the circuit principle. This figure shows that the

operation states of its current transfer are a very crucial property which is represented by the inductor current I_L. This technique is able to be isolated between the input and the output within different sides.

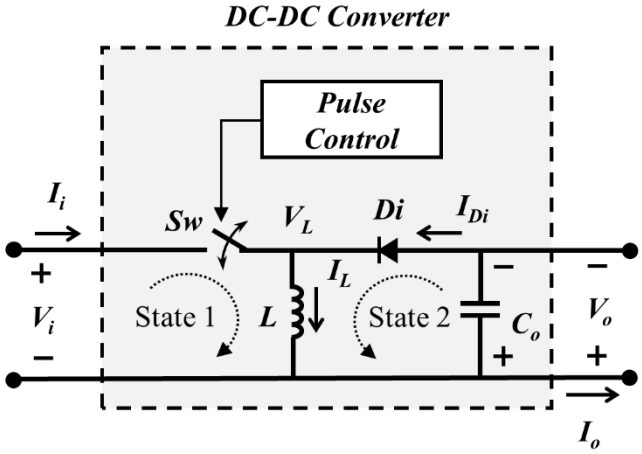

Figure 2.9 Buck-boost converter circuit.

The State 1 of the CCM corresponding to the charging process of the inductor L will be activated by *pulse control unit* connected to the switch *Sw* by conditions of the duty-ratio δ (δ denotes that the circuit is closed, the switch turns on T_{on}. (1-δ) denotes that the circuit is opened, the switch turns off T_{off}). The inductor voltage V_L is defined as a V_i, which is the piezoelectric voltage V. The piezoelectric current I can be represented at the same time by the input current I_i and inductor current I_L. This current is flowing through the switch *Sw* during the status T_{on}.

After the switch turns off T_{off}, the load resistance will be applied. In this state, the inductor voltage V_L becomes V_o. This output voltage V_o is to be the piezoelectric voltage V, which is applied to the load resistance or rechargeable battery in this system. Afterwards, State 2 of the CCM is completely employed on another side of the converter. The output voltage V_o is still drawn to the load from the inductor energy. The diode *Di* is forward biased due to the current direction of the State 2. The smooth capacitor C_o should be designed for its output current I_o as a low ripple signal. The diode *Di* should be also designed for the high-frequency switching devices as well.

Hence, the expression of the output voltage V_o as a function of the input voltage V_i and the duty-ratio δ is given by

$$V_o = V_i\left(\frac{\delta}{\delta - 1}\right) \tag{2.33}$$

Most applications in which a buck-boost converter may be used within the high-power consumption. The output current I_o of this system related to the diode current I_{Di} and the inductor current I_L is given by

$$I_o = I_L - I_{Di} \tag{2.34}$$

If the diode current I_{Di} reduces to the minimum value which is more than or equal zero, the optimum value of the inductor, $L_{opt,CCM}$, for the CCM can be written by

$$L_{opt,CCM} > \frac{R(1-\delta)^2}{2f_{sw}} \tag{2.35}$$

Hence, in the case of the DCM, the inductor current may be lower than zero. The optimum value of the inductor, $L_{opt,DCM}$, for the DCM can be given by

$$L_{opt,DCM} < \frac{R_{min}(1-\delta)^2}{2f_{sw}} \tag{2.36}$$

In this application, charging the rechargeable battery can be verified by these designed parameters to implement into the circuit technique. Therefore, the variation of the voltage output V_o as a function of the duty-ratio δ is able to be defined by this expression,

$$\frac{dV_o}{d\delta} = -V_i\sqrt{\frac{R}{2f_{sw}L}} \tag{2.37}$$

CHAPTER 3

DEVELOPMENT OF THE ANALYTICAL MODEL, OPTIMIZATION AND METHODOLOGY

This given justification in this chapter aims to propose the methodologies which support the modelling, in Chapter 2. The discussion of the research deliverables would be related to each other within these 3 chapters; from Chapter2 to Chapter 4. Moreover, two petty-patents (Muensit and Thainiramit, 2014, 2016) and one patent, which was written form this period, are related to this research thus illustrating the methodologies as follows:

3. Development of The Analytical Model, Optimization and Methodology

This research methodology chapter proposes a design and development of the energy harvesting technique as well as an implementation of the wireless device. The compressor outdoor unit is observed its vibrational characteristics thus being defined as a source of discrete vibrations. Therefore, the four main subtasks will be illustrated in this section by these followings: **(A)** ***The Energy Source Observation,*** **(B)** ***The System Design and Experimental Setup,*** **(C)** ***The Self-Powered Devices of The Batteryless Receiver and Their Device Configurations,*** and **(D)** ***The Energy Harvesting Implementation*****.**

3.1. Energy Source Observation

The selected direction is an air-compressor outdoor unit which is observed the characteristics considering as a vibrational source. According to the previous literature, Kim *et al* (Kim et al., 2015) confirm that the area upon the middle top of an outdoor-compressor structure is able to generate specific properties. For instance, these properties are particularly the mode of vibration, the resonance

frequency, and the maximum acceleration; the 2nd mode, 50 Hz, and 2.4 G were found by using the modified structure. Consequently, the outdoor-unit characteristic could be investigated by the vibration analyzer (Model 9080 Smart Trend Meter, TPI Inc., USA), as depicted in Figure 3.1.

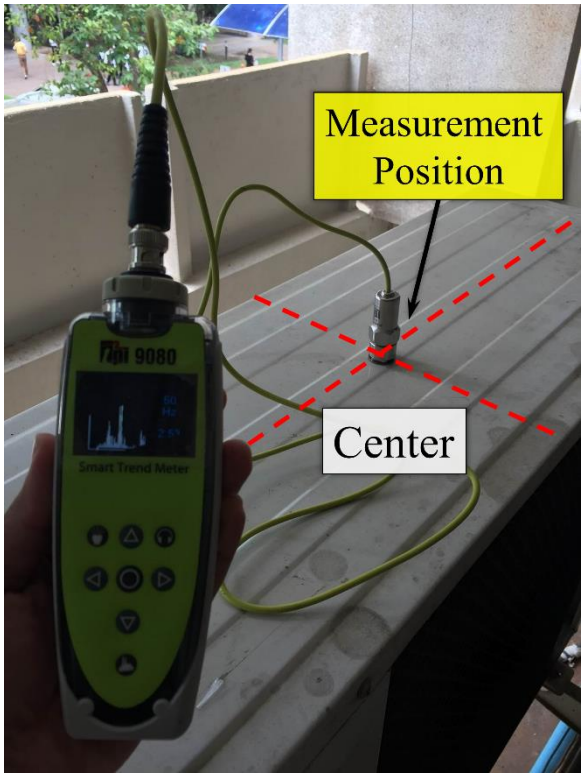

Figure 3.1 Acceleration measurement at the top-centre position of the air-compressor unit.

These both parameters are the resonance frequency and G value, shown in Figure 3.2 (measured during the fan blower running, at Physics building in Prince of Songkla University (PSU), Thailand).

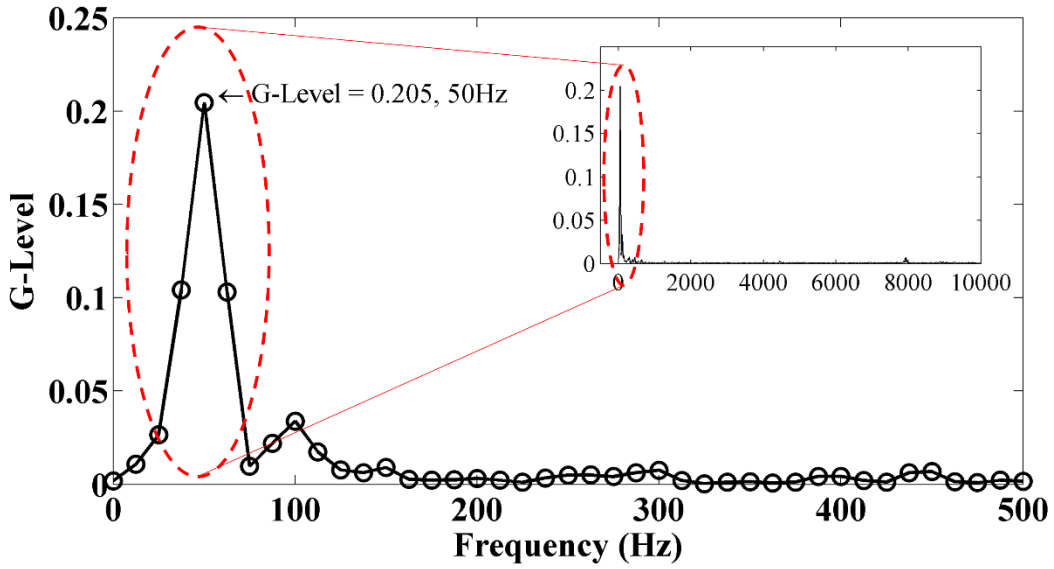

Figure 3.2 Frequency bandwidth from the vibration analyzer with the box inside (maximum-scale measurement from vibration meter) showing the wide-range scale.

The investigated parameters are shown in Table 3.1. The G-level of the systemic acceleration seems to be significantly lower than the paper reviews due to its air-compressor structure or the absorption architecture. Nevertheless, the frequency of this investigation seems likely to be equal to the mentioned literature. Indeed, these parameters show that around this area there is a high vibration zone upon the middle top of an air-compressor outdoor unit.

Table 3.1 Air-compressor outdoor unit parameters.

Parameters	**Value**
Operating frequency (f_i)	50.0 Hz
Acceleration (a)	2.007 m/s^2
G-Level (G)	0.205

3.2. Implementation on Air-Compressor Unit

Figure 3.3 illustrates the schematic of this system. The entire processes for the experiment could be presented by these next steps. To start with, the electrical power from the vibration is able to be transferred into the bank of capacitors (**Energy Storage**). The piezoelectric current can charge the capacitor bank by a traditional standard circuit (**Bridge Rectifier**). Thus, while the system was scavenging vibrations (**using the Energy Conversion**) from the energy-generator structure (**Air-Compressor Unit**), the interrupted process (**Switch**) could turn the switch off for allowing the current from capacitor bank (**Energy Storage**) to the wireless receiver (**RF Receiver**).

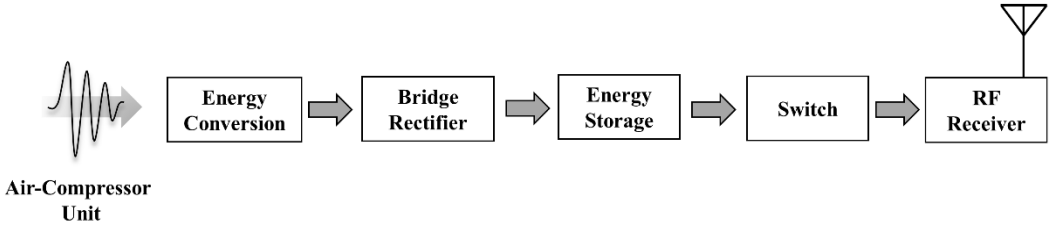

(a)

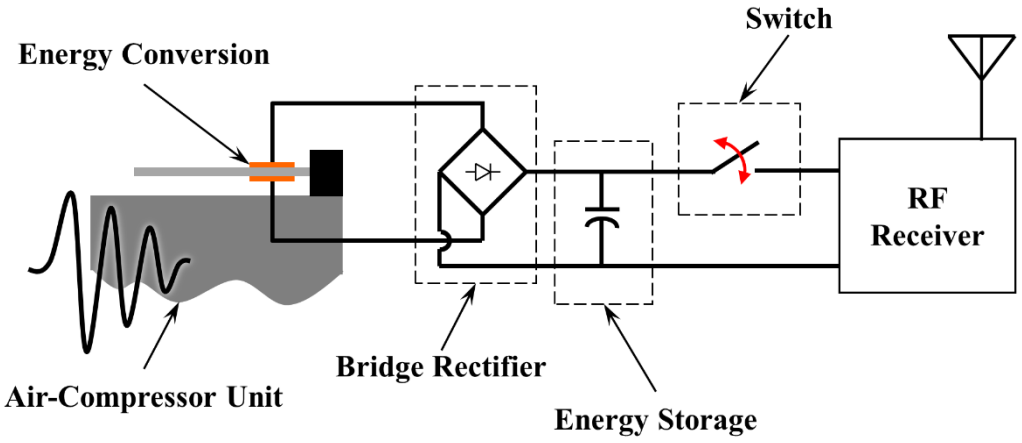

(b)

Figure 3.3 Diagram (a) and schematic of self-powered devices with battery-less for the radio-frequency receiver (b).

3.2.1. Energy Harvester for Air-Compressor Outdoor Unit

The appropriate-beam structure determined by Euler-Bernoulli beam theory is performed by the vibrating compressor. Accordingly, there is a smart element bonded on the beam where the element (a piezoelectric transducer: Kingstate Electronics Corporation, KPSG-100) is able to transform the mechanical energy into the electrical energy. The cantilever-beam structure with their fixed thickness related to the piezoelectric material could be created the whole design by these references (Davis and Lesieutre, 1995; Rakbamrung et al., 2010). The energy harvesting cantilever is installed at the specific area thus capturing the vibration at a near maximum resonance frequency. Therefore, the miniature power generator is operated under the extremely low G-level of the air-compressor outdoor unit. The vibrational harvesting structure as mentioned in this section is shown in Figure 3.4.

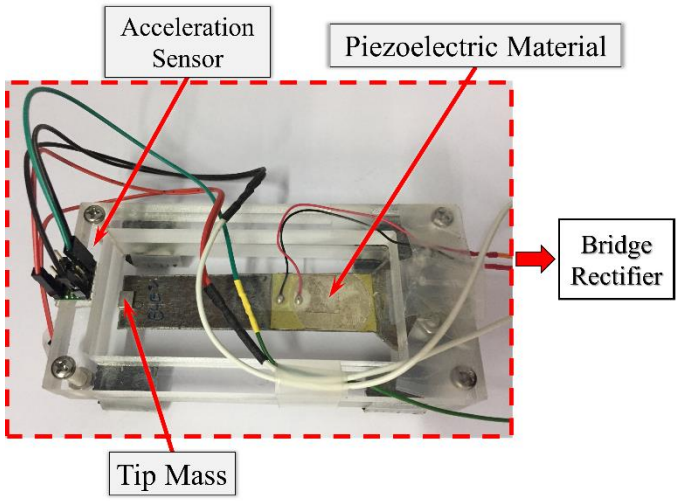

(a)

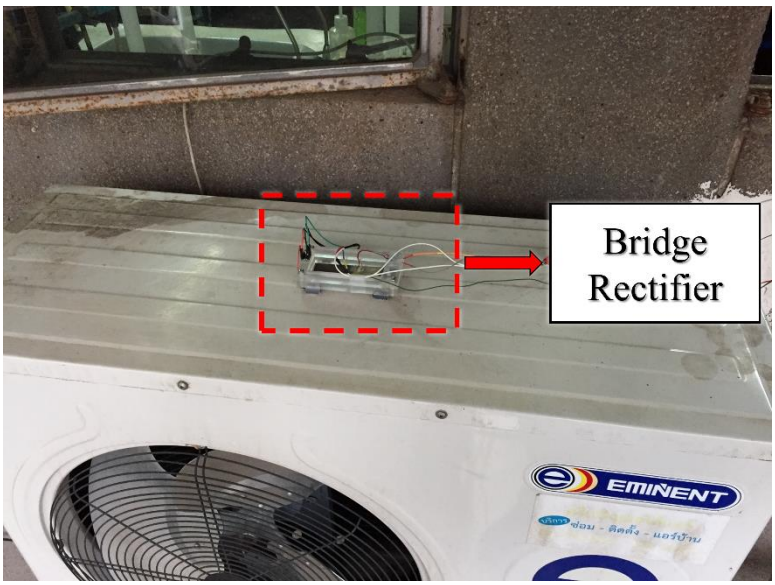

(b)

Figure 3.4 Energy conversion (beam structure) and structural components (a) at the harvesting area on the air-compressor unit (b).

3.3. Self-Powered Devices of The Battery-less Receiver and Their Device Configurations

The two key points of self-powered factors for sensor devices implemented low-power consumptions, which consume the electrical power from energy sources in case of the energy harvesting, are particularly regarding:

- Timing consumption (Tan et al., 2006), and
- Energy requirement (RFC Editor Organization).

3.3.1. Wireless Protocol

To start with, the timing consumption, having to configure both sides of the transmitter and receiver module is an important process for low-power-consumption devices within the implementations of the vibration energy harvestings. In this circumstance, the reconfiguration methods are actually implemented in the transmitter by re-coding the machine language inside the control unit. This unit is reprogramed the

functional coding for sending their encoded data from the client microcontroller (µ-controller or Microcontroller or MCU, i.e. Arduino-Uno-R3; using compatible board) to the receiver thus decoding the data by the server µ-controller (Sparkfun-Arduino-Pro-Mini, Low-power 8 MHz board).

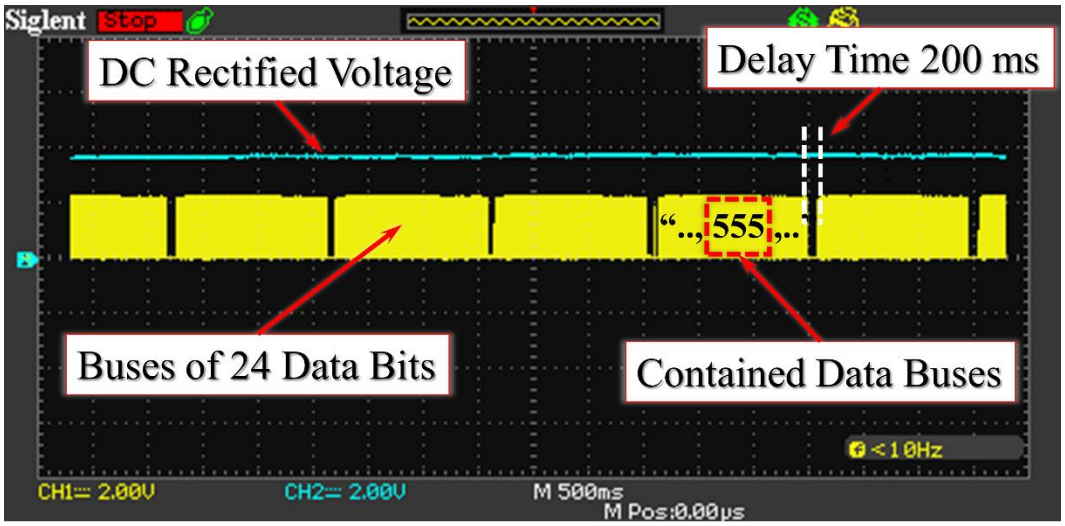

(a)

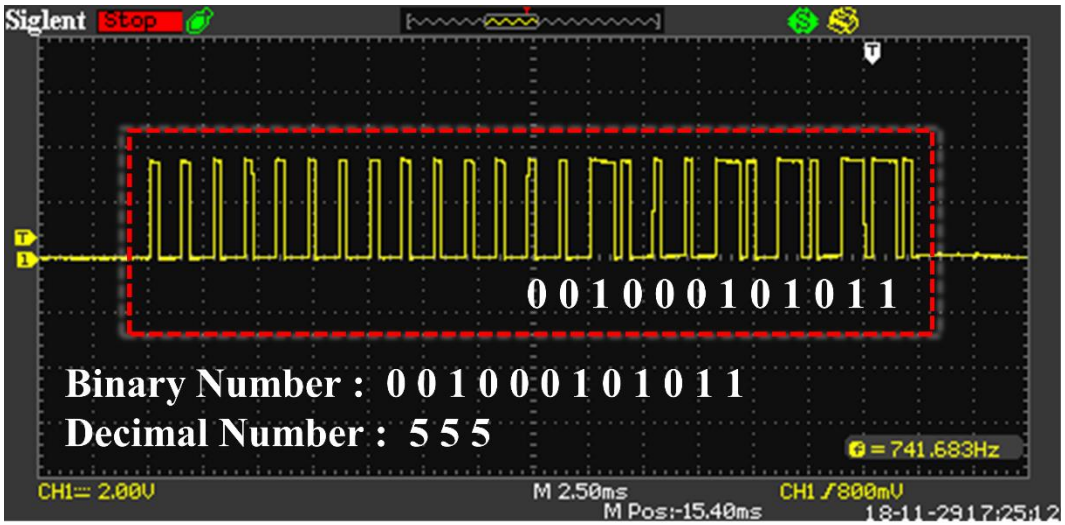

(b)

```
/* Format for protocol definitions:
 * {pulselength, Sync bit, "0" bit, "1" bit}
 *
 * pulselength: pulse length in microseconds, e.g. 350
 * Sync bit: {1, 31} means 1 high pulse and 31 low pulses
 *     (perceived as a 31*pulselength long pulse, total length of sync bit is
 *     32*pulselength microseconds), i.e:
 *      _
 *     | |_______________________________ (don't count the vertical bars)
 * "0" bit: waveform for a data bit of value "0", {1, 3} means 1 high pulse
 *     and 3 low pulses, total length (1+3)*pulselength, i.e:
 *      _
 *     | |___
 * "1" bit: waveform for a data bit of value "1", e.g. {3,1}:
 *      ___
 *     |   |_
 *
 * These are combined to form Tri-State bits when sending or receiving codes.
 */
```

(c)

Figure 3.5 Data-bus signal with the delay-time adjustment (a), and bits of data inside the data bus (b), and the format for protocol definitions broadcasting via wireless devices, ***captured from the RCSwitch.cpp code, thanks to the developer "Suat Özgür (sui77)", https://github.com/sui77/rc-switch/blob/master/RCSwitch.cpp*** [accessed: 15 June 2019] (c).

For example, these blocks of data after manual configurations by users are the encoded and decoded information based on the 24 bits protocol, to start with a synchronized bit, no address implementation, and reducing the delay time of the data separation from 1000 ms (millisecond) to 200 ms, as illustrated in Figure 3.5 (a) and (b); these are broadcasted by 315 MHz radio frequency from the transmitter device. And the protocol definitions are also presented in the following text box, as given in Figure 3.5 (c).

Another process of manual configurations for the energy requirement in this section is to focus on the electricity from the alterative power generator. Their electrical power is provided for the wireless receiver; the maximum current from the capacitor bank could start the receiver module to obtaine these buses of the transmitted data. Nevertheless, the data could be displayed on a computer screen through the TeraTerm Software (network communication software through the serial port). In the specific case, the energy consumption is involved the threshold of the electrical power to activate 1 block of the characters containing ASCII codes.

3.3.2. Wireless Sensor Node – Receiver Module Implementation

The final process, the piezoelectric current from the vibrating beam at near resonance frequency would be charged into the bank of capacitors behaving a power source for this receiver. The charging state is within average 3 minutes while the compressor of the air-conditioner was running a fan blower. The charging rate and the number of capacitors could be determined by the time-constant equation of the charge/discharge a capacitor. Therefore, Figure 3.6 illustrated the entire system of the harvesting energy implementation by discharging current inside the capacitors.

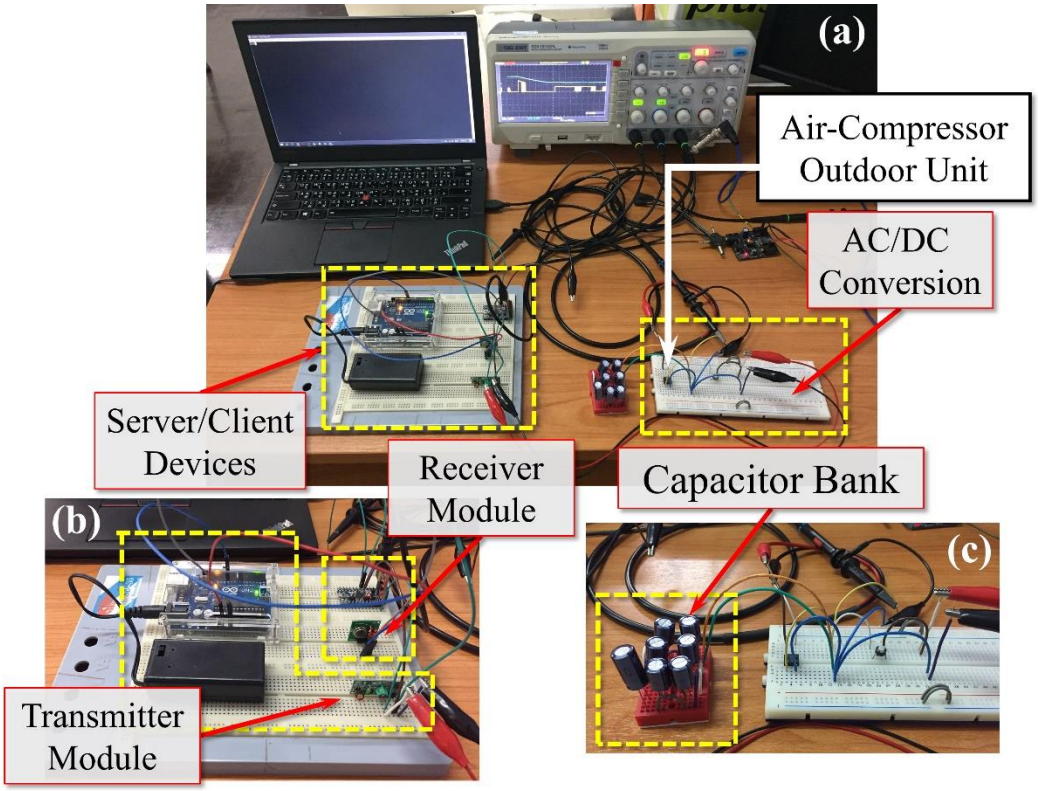

Figure 3.6 Experimental set-up for the self-powered receiver module (a), the transmitter and receiver module with connections of peripheral devices (b), and the capacitor bank connected with the bridge rectifier circuit (c).

3.4. Energy Harvesting Implementation and Experimental Validation

3.4.1. Experimental Set-up

There are two experimental set-ups in this research in order to support the direct and indirect force principle thus defining two types of a cantilever beam A and B. The cantilever beam A is implemented the direct force configuration to analyze the beam A characteristics, e.g. centre of gravity as a function of mass positions and a function of the number of masses with different positions. Another type, a cantilever beam B, is implemented the indirect force principle to capture the vibration upon the air-compressor unit. Then, the finalized implementations are demonstrated by showing the possible ability of future prospect in which the harvested electrical energy from piezoelectric materials can apply to the smartphone applications.

Figure 3.7 (a), the cantilever beam A is driven by an electromagnetic field from a coil of wire wrapped around an iron core as a solenoid (the solenoid, shaped like a cylinder with length), connected to a function generator (Siglent, SDG1010), which applies an electromagnetic continuous force into the magnetic tip-mass. A displacement sensor (Keyence Corp., IA-030 with the signal amplifier IA-1000) is used in order to monitor the beam free-end displacement. The displacement signal is observed by a digital oscilloscope (Siglent, SDS 1074CFL) reading the signal through the IA-1000. Moreover, the oscilloscope was also directly connected to the cantilever beam A due to the piezoelectric voltage measuring to detect the minimum and maximum voltage peak as a function of time. A multimeter (Fluke, Model 8840A) is applied to monitor a DC voltage which was measured parallel to the filter capacitor C (10 μF) throughout the diode-bridge rectifier (DF40M) with respect to the varied load resistance R.

The harvesting structure as presented in Figure 3.5 (b), would be characterized by the mass attachment regarding to different positions and the number of tip-mass to modify the resonance frequency of the cantilever beam A. The beam A was implemented a different type of piezoelectric patch connections, i.e. unimorph and bimorph beam (Thainiramit, 2012), in order to analyze the output power by comparing with two scenarios.

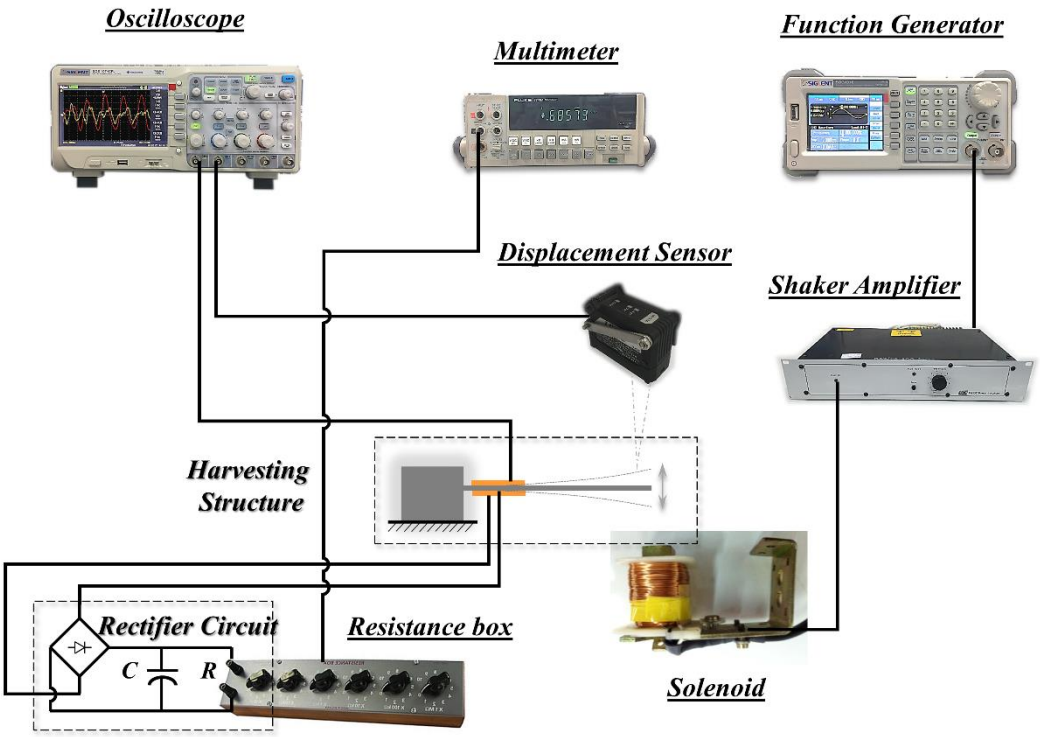

(a)

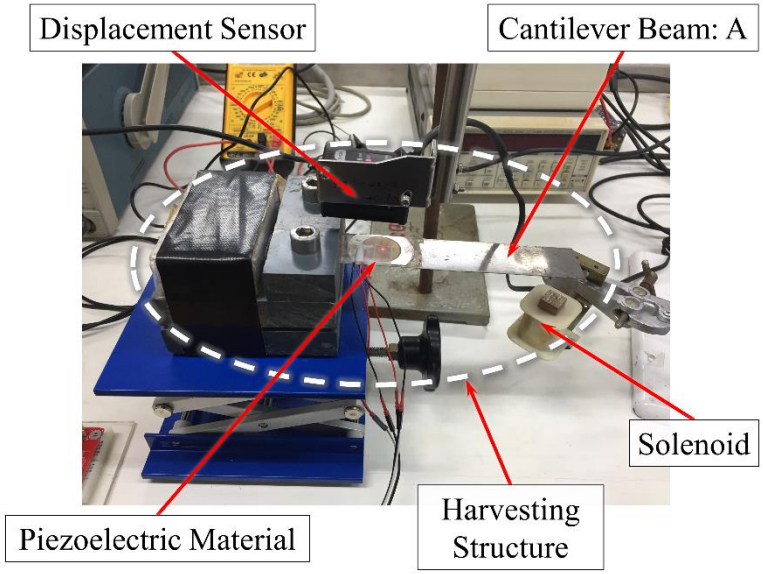

(b)

Figure 3.7 Experimental set-up diagram (a), and the harvesting structure (b) of the cantilever beam A.

3.4.2. Mechanical Tuning Methods

The mechanical tuning methods are divided into two schemes regarding the frequency tuning by moving the tip-mass positions and the added number of the tip-mass.

- The first purpose is to determine the piezoelectric voltage with respect to the moving positions of one tip-mass within different positions, i.e. 5, 10 and 15 cm (measured from the fixed end to the free-end side) in order to investigate the natural frequency variation, as described by Figure 3.8.
- The second purpose is to observe an effective factor of a spring stiffness by adding the tip-mass at each measured position, that is defined by measuring the mass position. The masses are added up to three maximums, as also given in Figure 3.8.

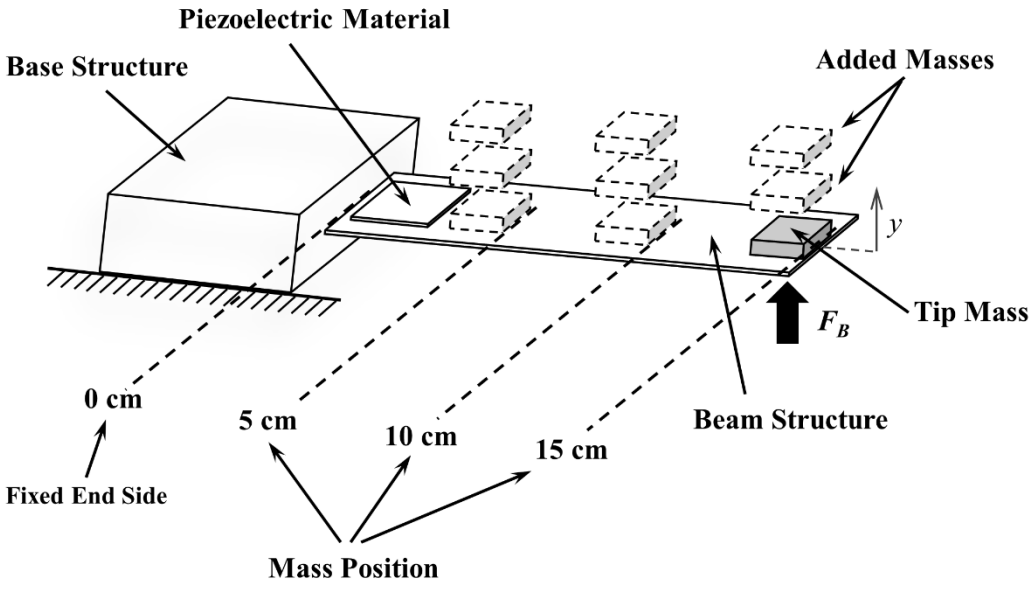

Figure 3.8 Natural-frequency tuning methods.

To take account of another experiment as the following Figure 3.9 (a), the instrumental measurement, i.e. oscilloscope, function generator, multimeter, bridge

rectifier circuit, resistance box and displacement sensor, are still used same as the first scenario yet the harvesting structure is changed to another type of beam structure, that is a cantilever beam B. The driven mechanism of the beam B is undergone by a shaker (LDS, V201 M4-CE), which generates vibrational energy by using amplified signal from a power amplifier (LDS, PA25E Power Amplifier).

Figure 3.9 (b) illustrates that the beam B structure is bonded on the shaker with an acceleration sensor at the fixed-end side while measuring the free-end side displacements using the displacement laser sensor. The tip-mass also corresponds to the G-level acceleration following the air-compressor investigation. In addition, the cantilever beam B would be operated under the measured resonance frequency as well. The theoretical comparison between the air-compressor and shaker harvesting power would be presented in the next chapter (Section 4.2, in Figure 4.2).

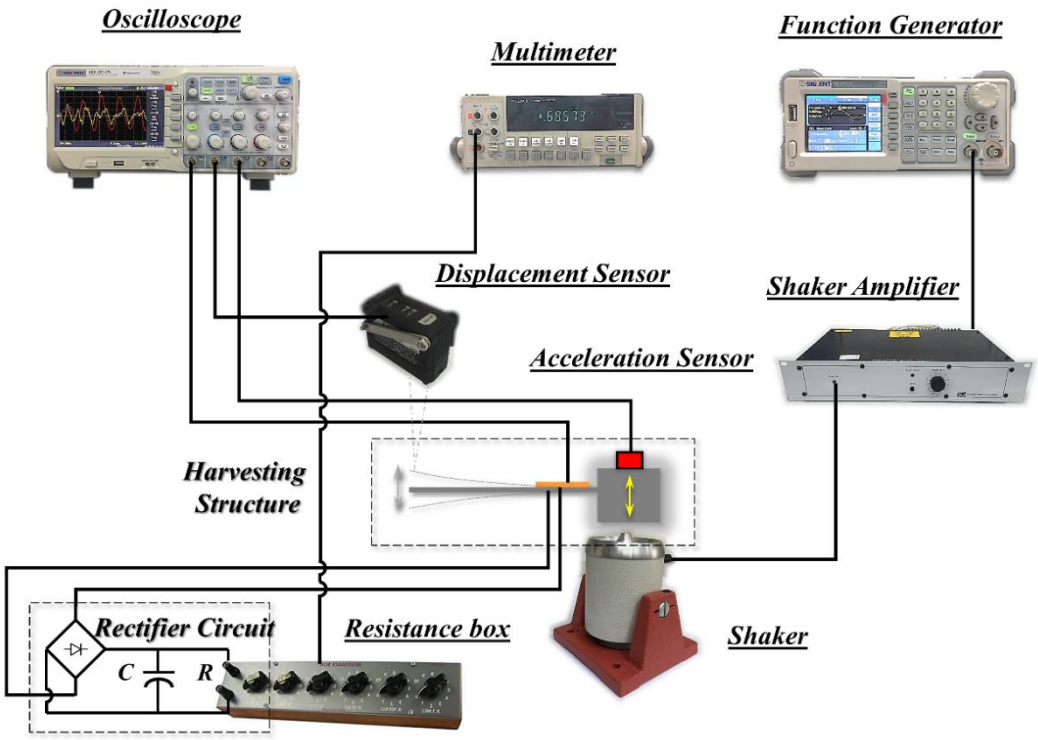

(a)

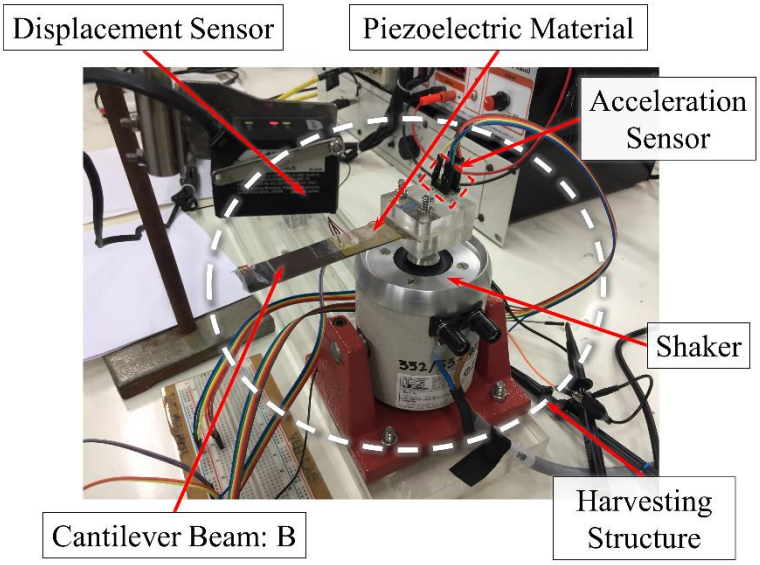

(b)

Figure 3.9 Experimental set-up diagram (a), and the harvesting structure (b) of the cantilever beam B.

3.4.3. Energy Harvesting Analysis

According to Chapter 2, the direct-force principle as proposed by Guyomar's research group who developed the electromechanical model and clearly described the lump-model of piezo-electromechanical principles contributes an idea to develop the indirect-force principle based on the d_{33} and d_{31} and other simple measurable parameters.

In terms of piezoelectric generators, regarding the indirect-force principle (section 2.2.2) and equivalent circuit model (section 2.2.3), appear to be well practicable with the final equations in the mentioned sections, e.g. expressions (2.28), (2.29), and (2.30). *In addition, the equation of governing vibrations (2.21) had arrived by substituting the real part of a rotating vector corresponding just to the real term in derivation processes.* Hence, the electrical power solution would also be validated to the DC power with respect to the constant vibration magnitude excluding the vibrational damping. The magnitude of applied force related to the displacement y thus following the condition of the electrical power solution is given by:

$$F_0 = \frac{M\omega^2}{Q} Y_0 \tag{3.1}$$

In many cases of energy harvesting applications and implementations, such a battery issue is the most important for the energy harvesting system. Due to the DC characteristic of vibration energy harvesting using piezoelectric methods, there are two subtopics to be presented in this analysis section as follows:

- **Rechargeable battery dimension**; even though the energy harvesting from vibrations using the piezoelectric method can produce a DC power, the electrical power from the material seems likely to be inadequate to supply a normal rechargeable battery. There are many types of rechargeable batteries to be able to address in various energy harvesting systems (Table 3.2). However, specifications of storages selected for employment as main or extended storages are the most significant to be considered. *The best solution is to manipulate an extremely low electrical energy, that is charged into the proper rechargeable batteries.* Chapter 2, section 2.3.1, provides the expression (2.36) to transfer the electrical voltage from the piezoelectric material into the specified rechargeable batteries throughout the enhancement circuit, and then the expression (2.36) was further determined their circuit abilities for the rechargeable battery dimension by yielding as the rewritten equation:

$$V_i = \frac{-V_{output,DC}}{\delta_{opt}\left(\sqrt{\frac{R}{2 f_{sw} L_{opt,CCM}}}\right)} \cdot \tag{3.2}$$

Where $V_{output,DC}$ is a charging voltage corresponding to the voltage across the rechargeable batteries as a function of the δ_{opt} with respect to the switch frequency f_{sw} and also the duty-cycle proportion δbased

on the piezoelectric current flowed through the inductor $L_{opt,CCM}$. The V_i and R link to the material properties corresponding to piezoelectric voltage and optimum resistance of the piezoelectric generator.

Table 3.2 General data of the rechargeable battery (Li, 2008).

Type	**Energy density (Wh/kg)**	**Power density (W/kg)**	**Round-trip efficiency, cycles, lifetime**
Nickel Cadmium	53	160	90, 1,500, 15 years
Nickel Metal Hydride	70	175	80, 500, 15 years
Lead Acid	50	200	78, 500-800, 8-10 years
Lithium Ion	160	1,800	95, 1,000, 2-3 years
Sodium Sulfur	85	115	75, 2,500, 15 years
Zinc Bromine	75	45	70-75, 2,000, 5-10 years

- **Scalable applications and the number of vibration harvester connections**; in addition to the rechargeable battery dimension, not only rechargeable batteries can be applied in order to be an electrical energy storage, but also the capacitor, such as a conventional capacitor and supercapacitor, could be applied to be the electrical energy storage for energy harvesting systems. Fortunately, in this research using both types of the storages, e.g. the specific rechargeable battery and capacitors, different applications were applied in this research as well. The rechargeable batteries are selected for use due to the conceptual validation regarding the direct force principle. *The rechargeable battery strongly delivers a steady output in the usable voltage; the voltage of the supercapacitor is evenly linear and drops from full voltage to zero voltage, but the capacitor rapidly decreases faster than the supercapacitor owing to the dimension and load resistance.* As a result, the capacitors are

certainly desirable to be considered for application as the short-term electrical power generator, as supported data in Table 3.3.

Table 3.3 Energy and power density (Li, 2008).

Device	Energy density (Wh/L)	Power density (W/L)	Life cycle (Cycles)	Discharge time (Second)
Batteries	50-250	150	$1\text{-}10^3$	>1,000
Capacitors	0.05-5	$10^5\text{-}10^8$	$10^5\text{-}10^6$	<1

Moreover, as proposed by the indirect force principle, to address multiple vibrational-energy sources that are available for an air-compressor unit with more than one unit, this methodology would be done by this given schematic (Figure 3.10).

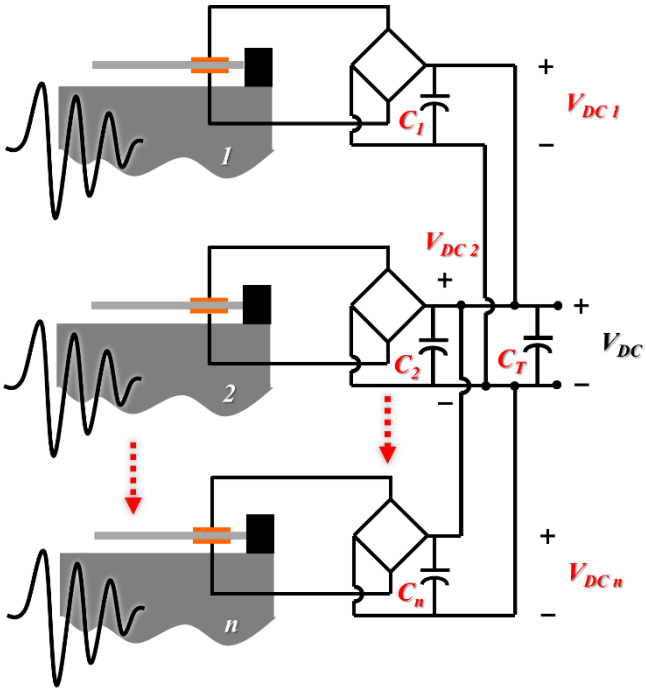

Figure 3.10 Multiple vibrational-energy source**.**

Thus, the equation described by Figure 3.10 in order to support the concept of DC-power generators based on the piezoelectric material

method (2.28), could be expressed by substituting F_0 from (3.1) into (2.28) then the finalized expression based on multiple vibrational-energy sources is given as follows:

$$\sum_{i=1}^{n} P_{IDF(i||...||n)} = \frac{V_{DC(i||...||n)}^2}{R_L} = \frac{\left(4d_{31} f_0\right)^2 R_L}{\left(1+4C_P R_L f_0\right)^2} \cdot \left[\frac{M\omega^2}{Q} Y_0\right]^2 . \qquad (3.3)$$

Where the DC-voltage output after a filter capacitor is denoted by $V_{DC(i||...||n)}$, and the piezoelectric power output from multiple vibrational-energy sources is represented by $P_{IDF(i||...||n)}$.

3.4.4. Energy Harvesting Optimization and Harvesting Power Validation

The energy harvesting power in this section would be analyzed by representing the normalized power. The two principles as proposed by the modelling in Chapter 2 will be discussed regarding the experimental set-up as well as supporting experimental results in Chapter 4 as well. Therefore, the beam structures should be measured by their electrical and mechanical parameters thus following the next step to analyze by using these system parameters, as given by Table 3.4.

Table 3.4 Mechanical and electrical parameters.

Mechanical parameters	**Value**	
	Cantilever beam A	Cantilever beam B
Beam length (*l*)	15.01×10^{-2} m	8.02×10^{-2} m
Beam width (*W*)	3.02×10^{-2} m	1.81×10^{-2} m
Beam height (*H*)	0.54×10^{-3} m	0.52×10^{-3} m
Dynamic Mass (*M*)	0.0257 kg	0.1166 kg
Structural damping coefficient (*C*)	0.087 N.s/m	0.994 N.s/m

Structural stiffness (K)	97.88 N/m	251.81 N/m
Resonance frequency (f_0)	17.6 Hz	47.5 Hz
Electrical parameters		
Piezoelectric capacitance (C_P)	166.84 nF	44.48 nF
Piezoelectric coupling factor (k_{31}^2)	0.7585	0.7588
Piezoelectric constant ($-d_{31}$)	41 pC/N	40 pC/N

Then, the electricity from the beam structure undergone under extremely low G-Level could be harvested thus attaching it on the compressor of air-conditioners. While a running state of the compressor was vibrating, the observed power could be determined by (2.28). Moreover, these two main parameters are the piezoelectric voltage and the load resistance is able to be linked to the optimal resistance and the maximum power as well, verified by (2.29) and (2.30), respectively.

3.4.4.1. Direct-Force Configuration Analysis

The output power is presented in Figure 3.11 by resulting in an overview of the theoretical approach. The graph summarizes that the normalized power exhibits the harvested power as a function of both the normalized load resistance and varied FoM parameters. The output power analysis would be illustrated in two main issues, which are described as an overview concerning the effect of the FoM, and the further effect over a high-power area discovered by enhancement circuit connections.

In general beam vibration, the generated power is proportional to the voltage and current magnitude of the piezoelectric generator to be dependent on the value of the load resistance. The load resistance maximizes the power at two peaks of the optimum resistance value depended on the FoM. For instance, the FoM relations is involved with the added mass (e.g. tip-mass, beam mass, and structural mass), the number of piezoelectric elements, properties of the piezoelectric materials, beam material, beam shape, structural dimension, and the attachment method while applying

on the harvesting structure. Besides, as given data by Figure 3.12, this figure presents the beat pattern while tuning the operating frequency of the cantilever beam B. When the masses are added to reach into a near resonance frequency (4 masses), the voltage signal from the piezoelectric material would be changed to the near steady-state vibrations. Indeed, the FoM parameters appear to be able to validate the structural frequency tuning as a simple process without any further enhancement circuit. And the expression, which is a typical example of beats as shown in Figure 3.12, is simplified the description as follows:

$$y_{DF} = C\left(\cos\left(\omega t\right) - \cos\left(\omega_0 t\right)\right). \tag{3.4}$$

Where C and y_{DF} is the damping coefficient of the cantilever beam A and beam displacement at the free-end side, respectively.

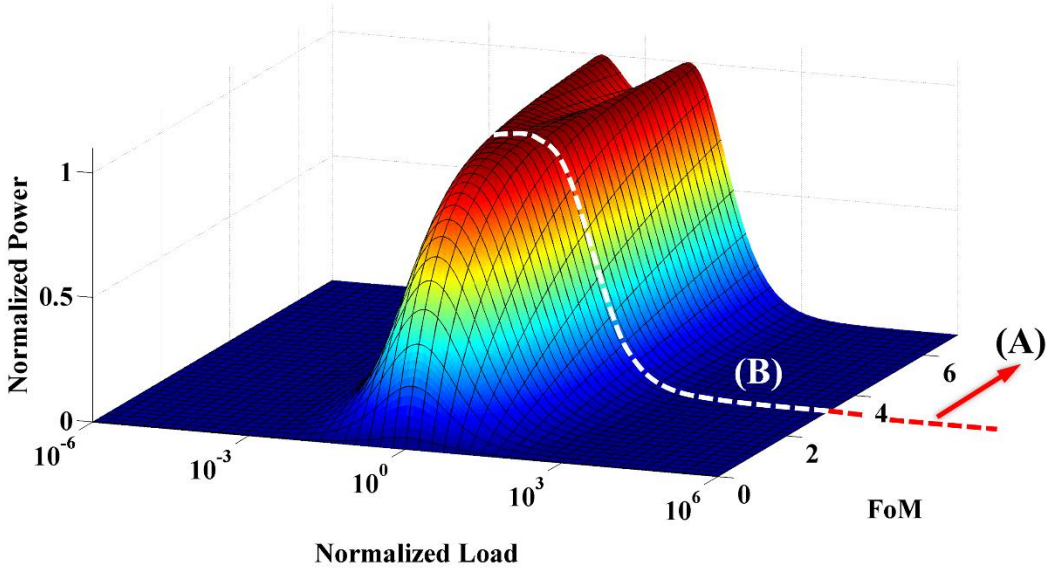

Figure 3.11 Direct-force normalized power as a function of normalized resistances, and FoM at operating frequency of harvesting structure, ***modified from Guyomar et al.'s equation*** (Guyomar et al., 2005).

In addition to normalized power regarding to the harvesting-structure tuning, this figure has also presented that a high-power zone regarding to the FoM factor focusing on a specific area over a white-dash line, that is labelled (B) (FoM is greater than or equal to 3). The output power appears to be expressed two peaks of the maximum power area (A) by the enhancement circuit (section 2.3.1). In this area could be accomplished by an effect of FoM by using a buck-boost technique (as also presented in section 2.3.1 and 3.4.3). Moreover, the result is strongly confirmed by an experimental output of the rechargeable battery charging; experimental results would be presented in section 4.3 of Chapter 4.

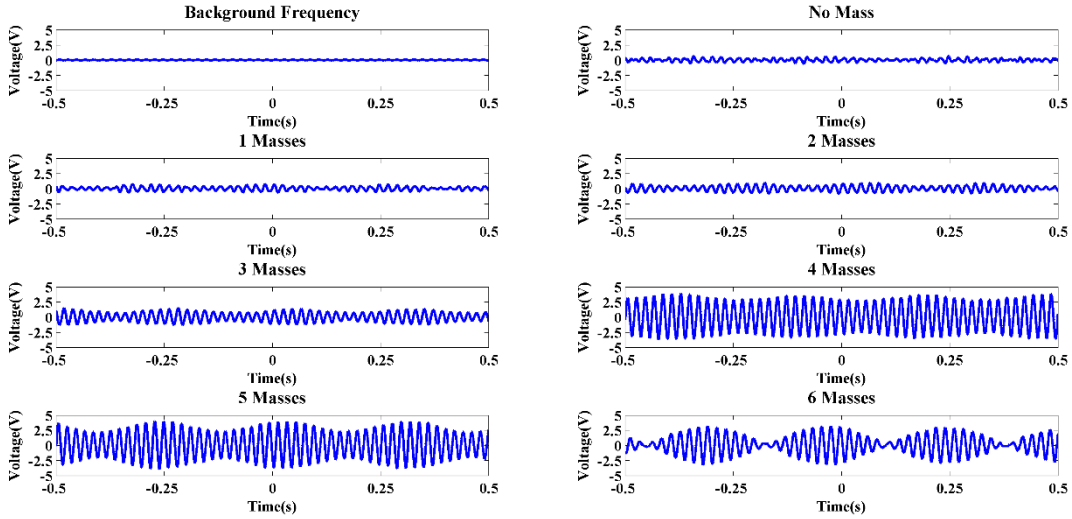

Figure 3.12 Transient phenomena of the frequency tuning method generating beat patterns

In conclusion, Guyomar's model seems likely to confirm that the theoretical validation is quite accepted with respect to FoM effects. The FoM parameters are probably responsible to be done for the whole normalized power representation; otherwise, further finding effects, that were in this study involving about to present the enhancement circuit abilities, are able to reveal another way for tuning and reaching the high power area by only using the buck-boost circuit.

3.4.4.2. Indirect-Force Configuration Analysis

In the last section of Chapter 3, the theoretical development is already accomplished by using simple parameters according to mechanical and electrical system parameters (Table 3.4). The indirect-force principle derived from another piezoelectric material variables (*T*, *E*) would be analyzed its electrical power by using the normalized power demonstration in this section. Moreover, due to these analyzed data being also exhibited the experimental results are in Chapter 4. The normalized power as a function of the normalized load resistance and quality factor (*Q* Factor) variations could be plotted then the discussion related to an observed experiment would be presented in this section. Before approaching to Chapter 4, there are three main issues to be considered: the indirect-force principle to be discussed what it is concerned about the electrical power with an effect of the frequency tuning, the further factors about a maximum power transfer, and the structural disturbance effects for this energy harvesting system.

The first analyzing focuses on the output power validations using the finalized expression with the condition of the constant-displacement magnitude Y_0 to predict an electrical power from the piezoelectric materials based on the indirect-force configuration. The equation (3.5), regarding the input angular frequency ω reached to the resonance angular frequency ω_0 by tuning the structural frequency, is rewritten from the expression (2.28) thus substituting by the equation (3.1) upon a constant input force F_0. As a result, the dependent displacement Y_0 and phase angle δ_1 upon the input angular frequency ω could be changed under these conditions. The phase lag increases from zero (at $\omega = 0$) to 180° (in the limit $\omega \to \infty$); it passes throughout the phase 90° at the explicit resonance frequency ω_0. Furthermore, the frequency out of this range upon the phase 90°, the displacement Y_0 is a minimum power same as the *Q* factor equal to 1; the maximum power is an ideal state, yet the experimental result was just plotted in this normalized graph as following *Q* equal to 35 as well. In fact, the white line appears to be shifted to the yellow-dash line, that is a resonance-frequency indication line due to the structural behaviour of the vibrational system. Figure 3.14 clearly confirms these phenomena as depicted:

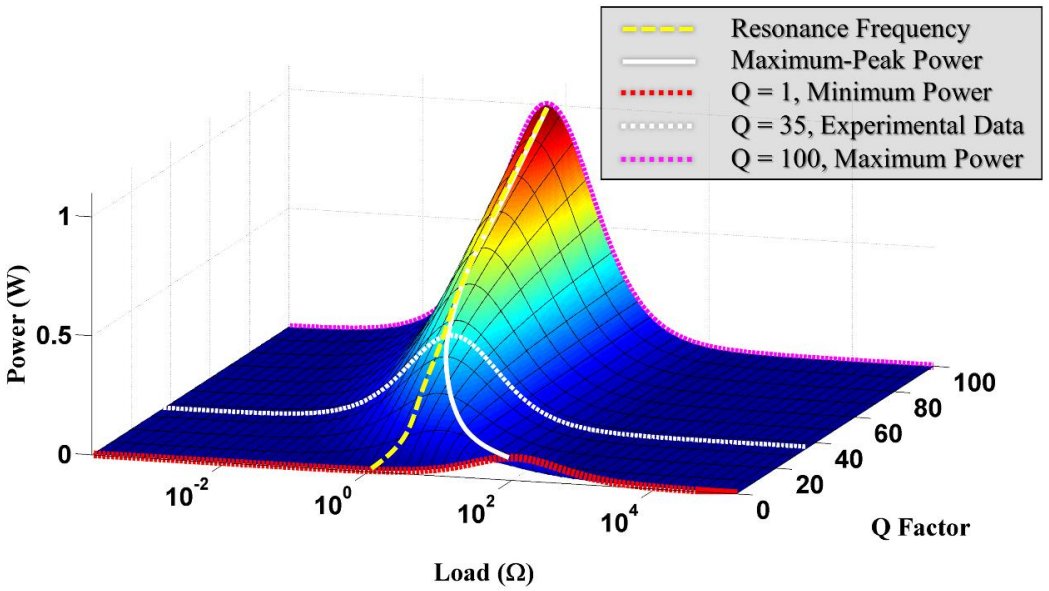

Figure 3.13 Indirect-force normalized power as a function of normalized resistances, and *Q* factor based on the modeling derivation of this dissertation.

And the expression of the electrical power in the case of the piezoelectric generator would also be written as (3.5):

$$P_{IDF} = \frac{V_{DC}^2}{R_L} = \frac{\left(4d_{31}\left(\omega_0/2\pi\right)\right)^2 R_L}{\left(1+4C_P R_L\left(\omega_0/2\pi\right)\right)^2} \cdot \left[\frac{M\omega^2}{Q} Y_0\right]^2 . \tag{3.5}$$

The second analysis, there are many factors for shifting and reducing the optimum load at the minimum power (red-dash line) due to an effect related to the *Q* factor. In this model proposes other ideas to validate the piezoelectric energy harvesting method and presents some evidence in order to confirm the effect of this structural analysis based on indirect-force model following this model derivation. Figure 3.14 (a) exhibits that the resonance frequency changing is proportional to a proof mass position that is the increasing of the structural frequency following the mass position moved to the fixed-end side of the beam. Furthermore, the piezoelectric voltage was somewhat

reduced by the beam stress at the near fixed-end side as well as the structural stiffness also being affected. Thus, the beam displacement at the free-end side is slightly changed into a lower magnitude of vibrations.

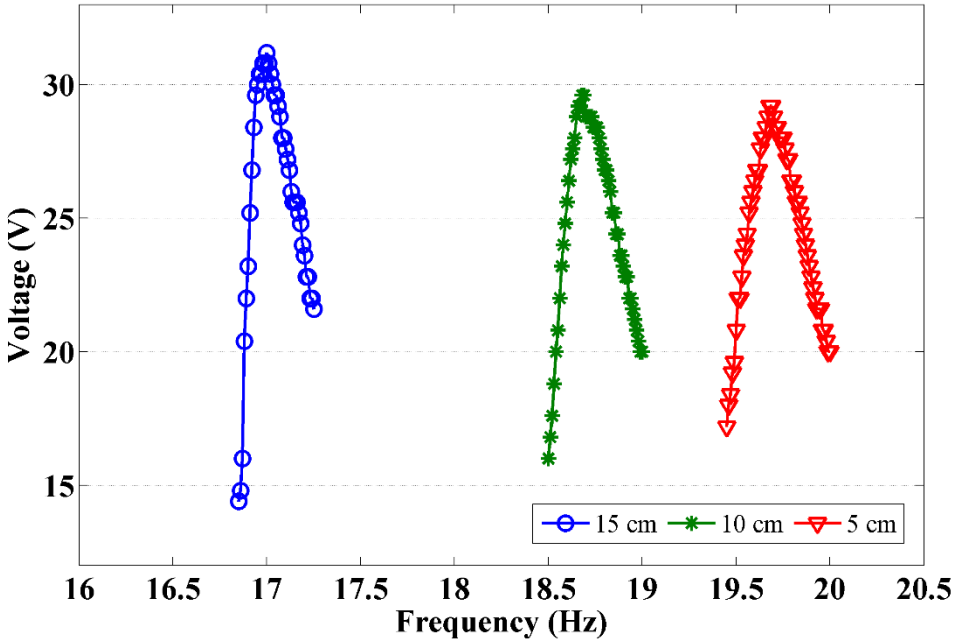

(a)

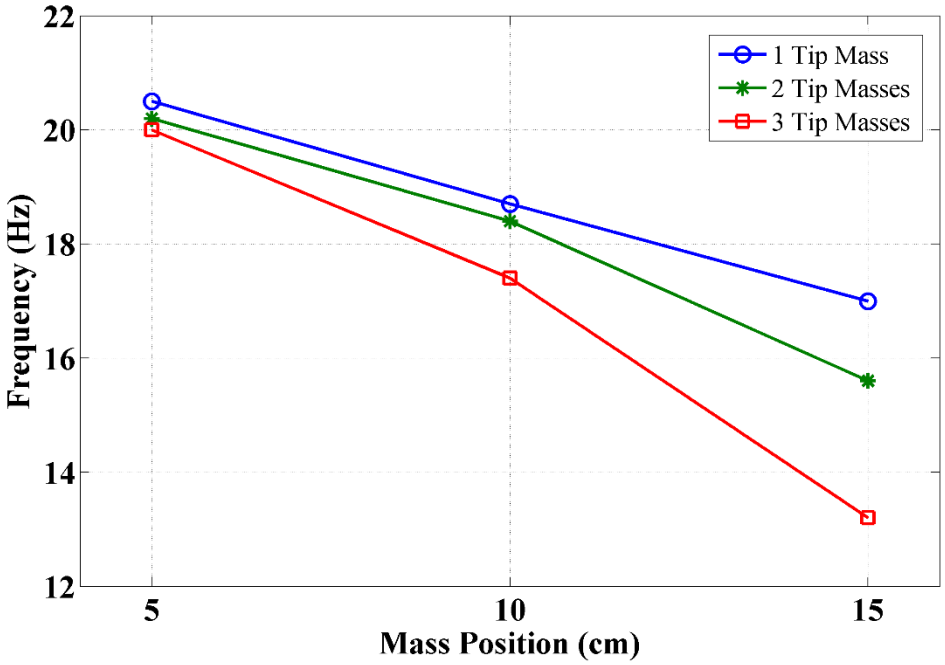

(b)

Figure 3.14 Experimental results present the deliverable of the structural-disturbance phenomenon, (a) one proof mass applied and (b) one, two and three proof masses applied upon the same mass bonded positions.

Coincidently, in the case of more than one induced vibration regarding to the systemic disturbance, (i.e. further peripheral components, bonding method between the energy source and harvesting structure, and proof masses on the beam structure), might be potential to force the harvesting and ambient structure absolutely into differences natural frequency. And also the magnitude of vibrations on the beam structure upon ambient structures would be shifted as well. Another, Figure 3.14 (b) would be presented that the number of proof masses is inversely proportional to the natural frequency of the harvesting beam as well as dramatically increase by the proportion of the number of masses and applied position to the free-end side.

Finally, in addition to an analysis of structural parameters and perturbation factor corresponding to the harvesting structure, further significant factors of vibration energy harvesting based on this research have been found that internal resistance of power generator sources, such as the resistance and capacitance of the material, diode, and filter capacitor, affects to the optimal resistance; moreover, beam

types (i.e. unimorph and bimorph beam), as well as natural frequency of the harvesting structure, also make the optimal resistance of the harvesting system change by shifting the optimal load value followed by input resistance of piezoelectric generator as mentioned model in Topic 2.2.3. In this case, Figure 3.15 illustrates that piezoelectric power as measured from unimorph (a) and bimorph beam (b) is dramatically different because the bimorph beam is bonded by two material at top and bottom near the fixed-end side of the harvesting structure. Therefore, their affect to the beam stiffness then reducing the fixed-end side strain even though the free-end side is vibrated as the same displacement when comparing with controlling the condition of experiment circumstances. Indeed, Figure 3.15 (a), and (b) appear to confirm the effect of internal resistance and beam stiffness regarding the optimal load resistance and piezoelectric voltage magnitude, respectively.

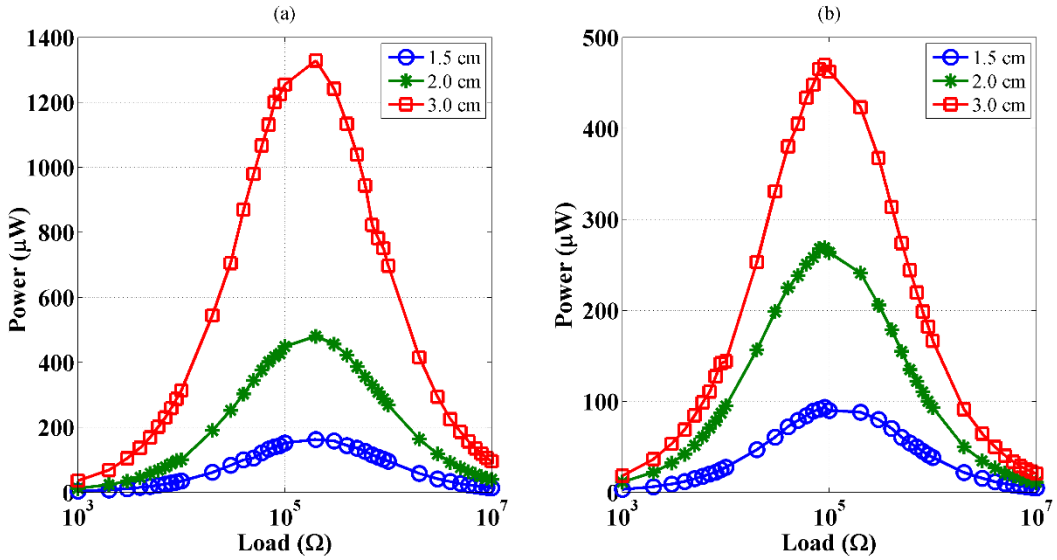

Figure 3.15 Electrical power of two-different-configuration piezoelectric beams as a function of free-end side displacement (i.e. 1.5, 2.0 and 3.0 cm), (a) unimorph beam, and (b) bimorph beam.

On the whole ideas, Indirect-force principle could be potentially validated by confirming the experimental results in Chapter 4. Ambient effects acting into the natural frequency and structural properties of the harvesting structure are the most definitely important for designing the vibration energy harvesting system.

Moreover, the highest power of vibration energy harvesting could be accomplished by reducing and avoiding the disturbance effects as proposed by *Q* factor references in these mentioned discussions.

CHAPTER 4

RESULTS AND DISCUSSIONS

4. Results and Discussions

4.1. Introduction for Summary Chapter

This Vibration Energy Harvesting system is started by the validation of a cantilever beam where it is measured the electrical power compared with the theoretical result by these yielding expressions (2.28), (2.29), and (2.30); then this powered extraction from the piezoelectric cantilever vibrated on the air-compressor unit is directly charged to the bank of capacitors instead of acting as a smoothing capacitor to prevent the rippled current. It is connected after the rectifier circuit (Standard Circuit interfacing) followed by the electronic switch. Even though the enhancement circuit could be omitted to connect this system, the charged accumulation appears to be fully charged by conventional interfacing circuit. As a result, this experiment was to be observed then analyzing these following results as well as adding more support results based on the enhancement circuit and further applications on the smartphone in order to access the temperature data.

4.2. Electrical Power

According to the equation (3.5), Figure 4.1 was plotted by the different load resistance followed by these parameters, as given in Table 3.4. This overall trend could be analyzed by comparing the measured result from the experiment, during the running state of the flowing fan inside the compressor unit. Therefore, the dot graph of the experiment is seemed likely to confirm by the theoretical result as mentioned above (3.5), but these are a slight shift when comparing the maximum peak of both graphs. These experimental results are probably influenced by the optimal load (optimal resistance) corresponding to the inside resistance of the standard interface, filter

capacitor for DC circuit and piezoelectric materials. Furthermore, the error identifications appear likely to indicate that the power at near maximum is dramatically higher than the low (1k – 10kΩ) and high (1M – 10MΩ) resistance because the cantilever beam is operated at near resonance. The instability signal induces a ripple current which affects the filter capacitor, and the fluctuated current levels within the capacitor could not be measured in the DC signal stability.

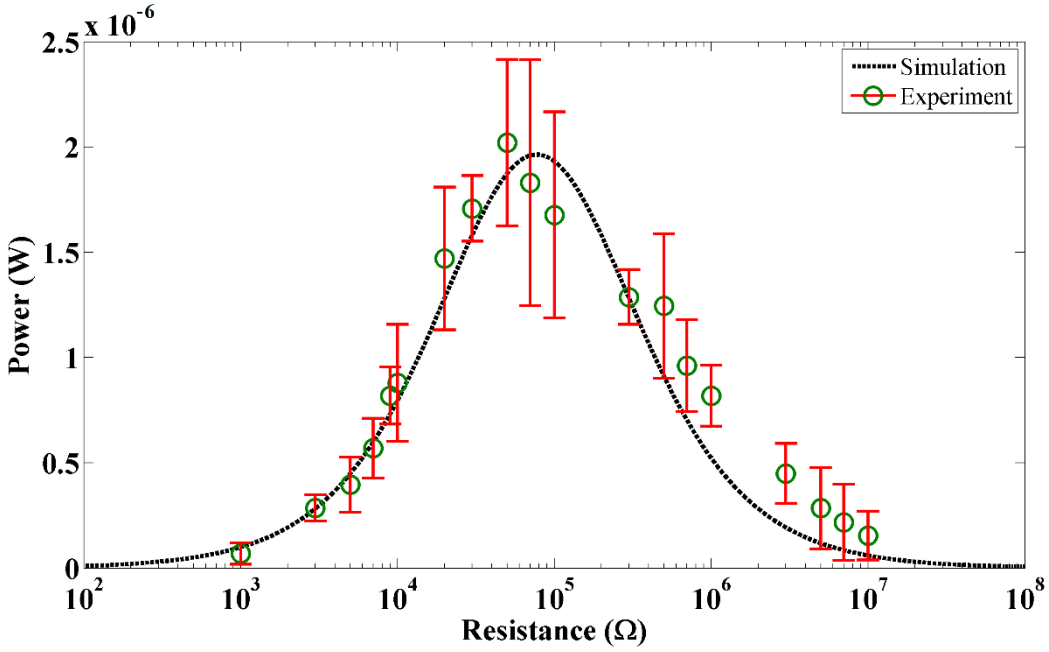

Figure 4.1 Piezoelectric electrical power from the air-compressor outdoor unit.

Furthermore, when comparing between the laboratory measurement and practical harvesting circumstance on the air-compressor unit, the harvesting power from the laboratory demonstration using the precision shaker to control the vibration and acceleration is noticeably different from the realistic situation implemented on the air-compressor unit. The electrical-power measurement (Figure 4.2) is to present the main inferences linked to the measured result thus validating the theoretical approach as reported upon the equation derivation and theoretical analysis in Chapter 2 and 3, respectively. This experimental result reports that the measured result (A), in Figure 4.1 and 4.2, is undergone by the condition of low *Q* factor due to the operating frequency depended on the harvested structure, proof mass and bonded method between the energy harvesting structure and vibrational energy sources. In addition, the acceleration magnitude induced by the vibrational energy source, which is an air-compressor unit, in this case, is probably reduced by the mass weight of harvesting structure. Significantly, these effects are directly related to the electrical power by changing the *Q* factor. As a result, the laboratory result (B) is dramatically distinct around 7.42 times from realistic applications on the air-compressor unit even though many factors are controlled. In fact, this result (A), and (B) is truly followed the theoretical derivation of this research development although the shifted peak of the graph (A) is on the left of the graph (B) because of the boundary of the theoretical validations.

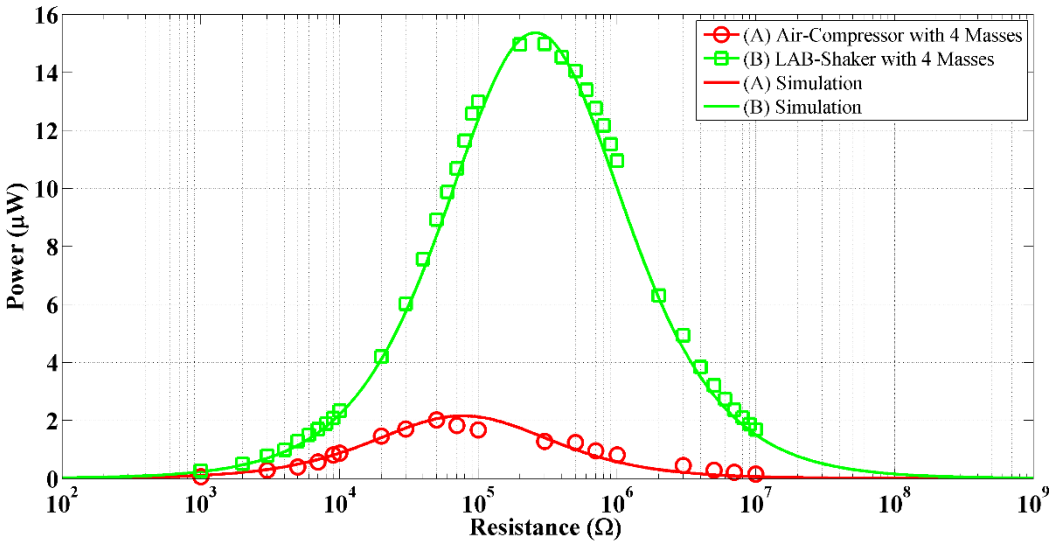

Figure 4.2 Comparison of the air-compressor harvesting with the laboratory measurement by controlled vibrations and accelerations using the shaker.

In addition to the verification of the electrical power, the miniature generator is to be a power generator using the piezoelectric ceramic under particular conditions: low G-Level, low piezoelectric constant ($-d_{31}$ = 40 C/N), and low output impedance (unnecessary to use a more enhancement circuit for charging). These results (Figure 4.3) demonstrate that the potential ability of ultra-low power generators appears to be able to charge a small capacitor throughout a larger dimension, as depicted their system connections in Figure 3.6.

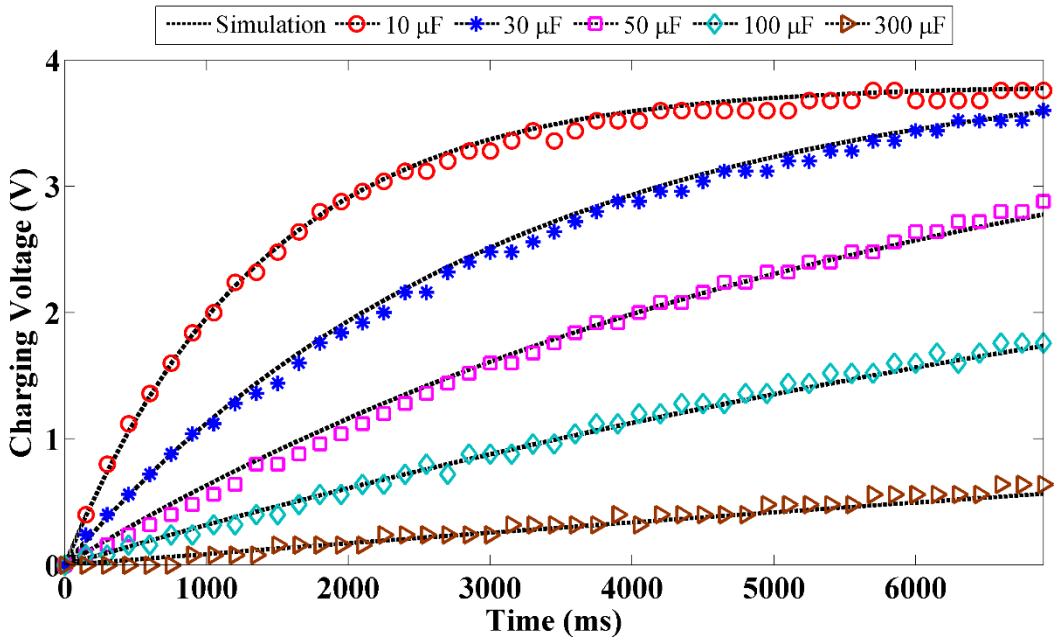

Figure 4.3 Piezoelectric voltage while charging the capacitor of various dimensions.

In conclusion, the limitations of this section have already been discussed in this context section including the suggestions of controlled variables. These factors are able to use the equations developed in this dissertation as a tool to predict the practical situations. And the *Q* factor is also able to be optimized in order to reduce the error number and even improve their system by following these experimental results as a study case for the structural design of the vibration energy harvesting system using the beam structure.

4.3. Power Enhancement Circuit

This section describes the result of the experiment in terms of the electrical power produced from the buck-boost circuit. This circuit is able to charge a rechargeable battery with an appropriate FoM value. The results confirm that the output is coming from the enhancement technique, which is able to be applied in the high-performance power range and the FoM value greater than 2.5 was found when using the switching technique, as shown in Figure 4.4 (a) and (b). In addition, these results appear to indicate the importance of energy loss 76 per cent in this buck-boost circuit (Figure 4.4 (c)). The harvested power is absorbed by this enhancement circuit up to 4.2 times. Therefore, an applied electrical power received from the piezoelectric material using bimorph beam configuration could be accomplished with only two displacements, (e.g. 2, and 3 cm) due to the output power increasing by the beam displacement induced from vibration magnitude.

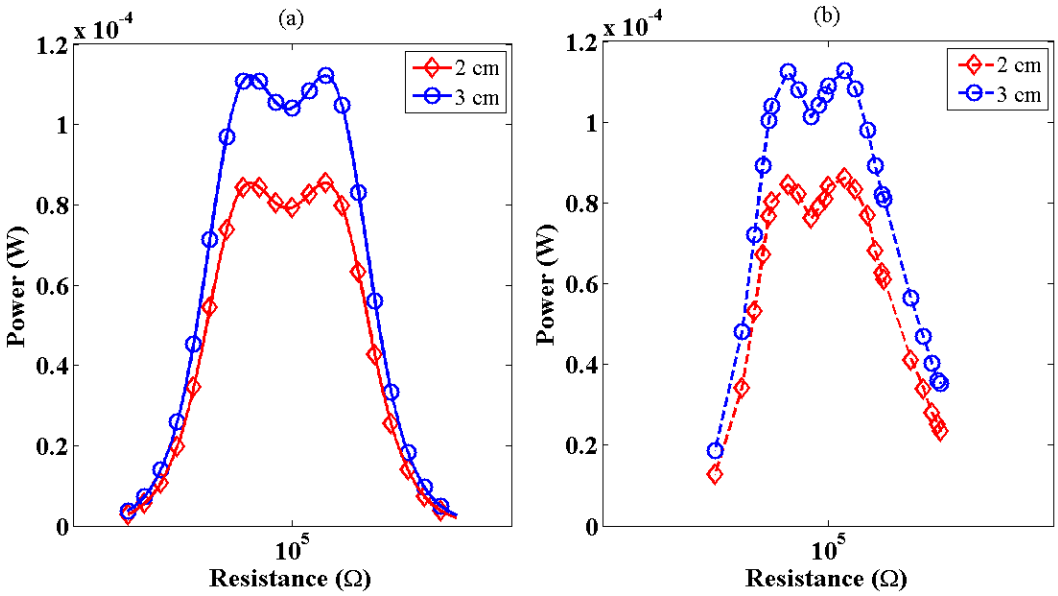

(c)

Figure 4.4 Experimental (a) and theoretical result (b) from harvested power using the DC-DC converter circuit, and (c) this DC-DC converter circuit is so-called Buck-Boost Circuit to enhance electrical power transferring into the specific rechargeable battery.

Figure 4.5 shows the results in terms of the voltage and current supplied to the rechargeable battery when it is fully charged. This result was obtained under CCM conditions and also followed the minimum-starting-state rule for the charge accumulation into the rechargeable battery.

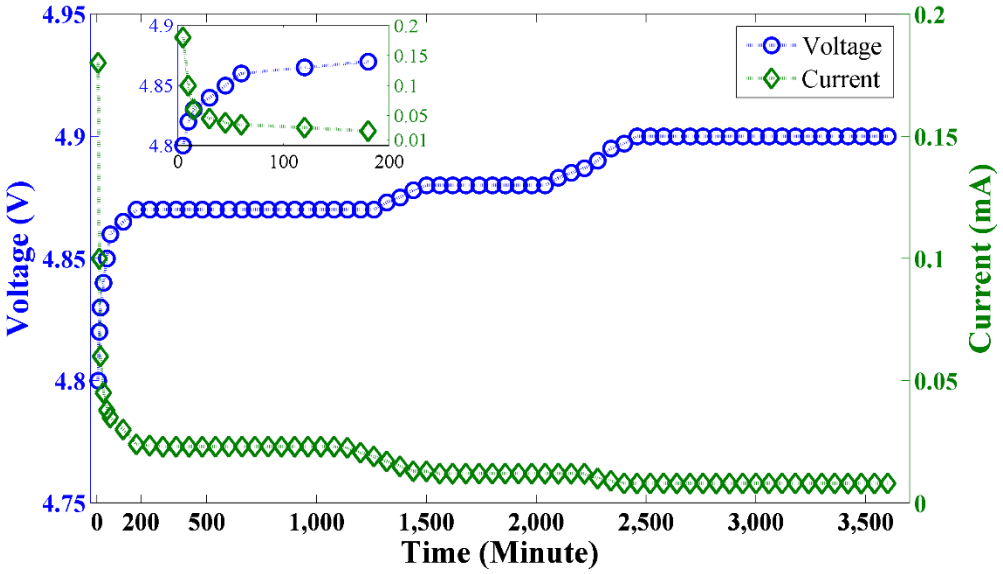

Figure 4.5 Voltage and current measurement of the full-charging state as measured on a rechargeable battery, small box inside showing the zoomed scale at the beginning state.

To summarize, the enhancement circuit (Buck-Boost Circuit) seems likely to be well functional working as a rechargeable battery using the specific type. The proper mode of driving the circuit should be used the CCM condition because this mode is able to keep the stability current in the circuit consumption. Then, the transfer current after this enhancement circuit would be able to charge the rechargeable battery by using the trickle current condition. However, this circuit is designed by selecting the ultra-low power consumptions of any devices. The circuit can be optimized and redesigned for the suitable parameters in order to be the vibration energy harvesting circuit for another dimension of specific rechargeable batteries.

4.4. Energy Harvesting Implementations Based on IoT Connected to Smart-Phone or Wireless Devices

In practical implementations, the finding implementation of vibration energy harvesting on the compressor of air-conditioner units without the enhancement charging circuit is probably related to the time constant of capacitors due to their application regarding the discrete vibration operation. In order to be an extremely-low-power generator for extremely-low-power devices could be shown its result in Figure 4.6. These transmitted data from the transmitter could be done by presenting the result on the computer screen after decoding the specific data. In the discharging circumstance of the capacitor, the solution might be done within average 500 ms, and this appears to be supported by the proper size of the capacitors because the voltage across devices should be higher than the operating voltage for the reading logic state that is dependent on each device.

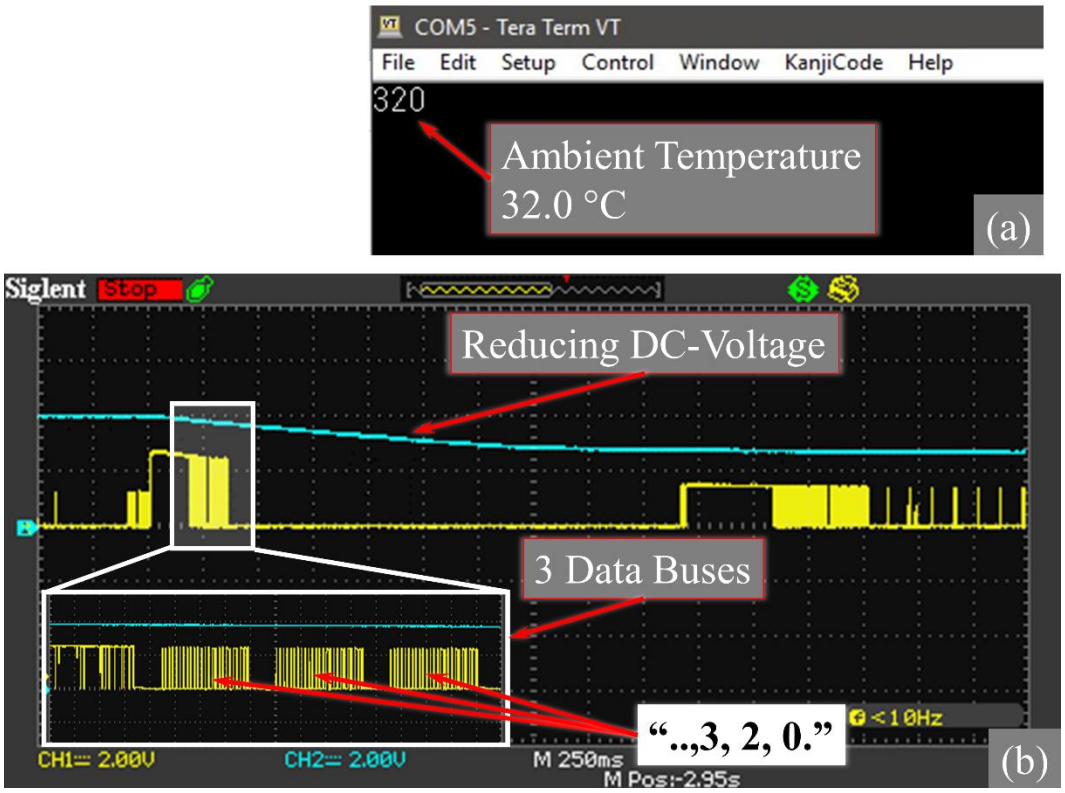

Figure 4.6 Decoded output data displayed on the computer screen through serial port communications (a), the DC-voltage by using the temporary voltage from the capacitor bank discharging to the receiver module (b).

In order to achieve the implementation of the receiver, the experimental results were done by the full bank of capacitors. The parallel connection with adding the different dimension of capacitors up to the average value of 3,150 µF significantly needs 4 V of self-contained voltage for a discharging state. The charging voltage of a capacitor bank from start (0 V) by running an air-compressor unit could possibly be accomplished by the average 52.50 minutes; hence, the running state of the air-compressor unit is able to be done within 18 loops of the compressor operation. These are the status of the air compressor to run and stop blowing fan (ventilator unit). The charging current would respectively be started and stopped by the turning on and off the electronic switch during the operation of air conditioners. The device could read such busses of the data, which contain 72 bits of characters.

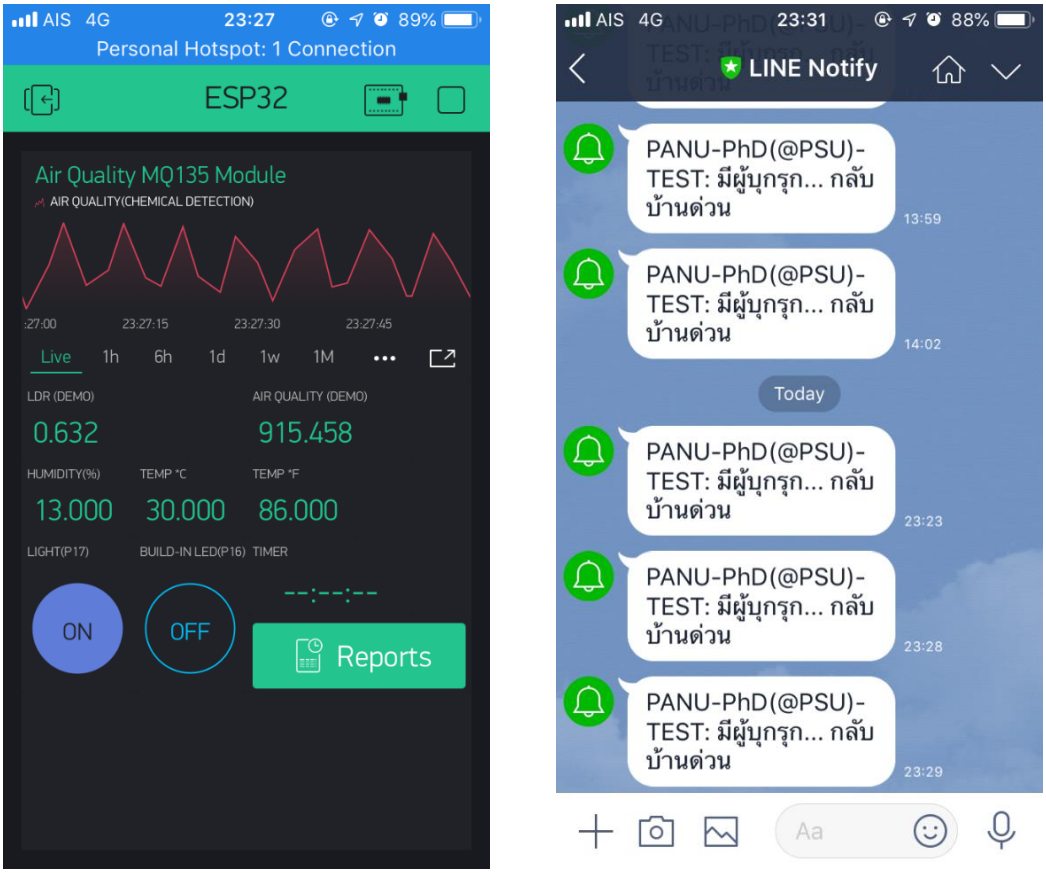

(a) (b)

Figure 4.7 Mobile application powering devices by the electrical power from the vibration energy harvesting using the piezoelectric methods.

Chapter 4 summarization using Figure 4.7 to be presented the applications of these whole experimental results, as depicted in this Figure 4.7 (a); this Figure is to be illustrated the mobile applications (supported IOS & Android OS) receiving the ambient temperature from wireless receiver module tested in this research. And another Figure 4.7 (b) is to be presented the alert signal through the Line Message via a smartphone screen by configuring the program coding inside the flash memory of the microcontroller. These results obviously confirm that the vibration energy harvesting using piezoelectric method could be replaced the batteries or other energy sources by using the conventional capacitors which are properly designed for matching to its applications; furthermore, these results are also strongly confirmed by its practical applications from environmental parameters using the free-vibration with the piezoelectric energy harvesting method.

CHAPTER 5

CONCLUSIONS AND FUTURE WORKS

5. Conclusions and Future Works

5.1. Main Conclusions

This enhancement circuit focuses on the optimization of the power from a directly applied force on a piezoelectric device. The energy harvester converts ambient vibrations into electrical energy and the piezoelectric generator as the specific power source for a rechargeable battery. The power optimization was based on the equations relating to piezoelectric materials, especially the piezoelectric generator equation. These electrical circuits composed of a full-wave rectifier, a capacitor for smoothing the voltage, the DC-DC converter technique and various resistors. In this study, the switching technique used a buck-boost converter, which has the appropriate properties to optimize the power based on the relationship between the input voltage and the input current. This device was able to fully charge a 150 mAh, rechargeable battery in 40 hours due to the properties of the piezoelectric material and harvesting structure corresponding to the FoM. This piezoelectric generator can act as the electrical power source for electronic devices using a low power system and the characteristic charging graph confirmed the charging capacity of the buck-boost circuit. However, this technique is not suitable for use with a low applied force or a low electromechanical coupling factor and the circuit's intrinsic properties must be defined for power optimization. Furthermore, the power consumption of the buck-boost circuit can easily be minimized, and the circuit requires neither sensors nor a sophisticated algorithm.

However, in the research objective based on the vibration harvesting energy, the discrete vibration form ambient sources in this research coming from an air-compressor is proposed as a key point. Moreover, this dissertation employs a conventional buzzer as a transducer for being a main coupled material. The vibration is harvested by a cantilever-beam structure bonded to the piezoelectric disk. Its mechanical energy from the vibrating-energy source is transformed into the electrical

energy. Output energy is stored in capacitors which are connected in parallel as a bank of capacitors to be an energy ignition by their energetic threshold. These scenarios are the conventional idea on the state of the art in piezoelectric energy harvesting. However, of great concern are the implications of the global impact for many countries using the air-conditioners. Especially the implementation, the controller of the wireless transmitters is not only rewritten the code inside its programing register in order to change the transmitted data, but the wireless receivers should be also reconfigured for their proper functions by rewriting the code as well. These results confirmed that a traditional cantilever (beam structure) could act as a charger for the connected capacitor which was subsequently an energy source to drive these wireless units. In this research scheme, a running air-conditioner produced a charging cycle then applying the converted electricity into the 3,150 μF capacitors within 1 hour. This dimension is sufficient to send and receive the data of the atmospheric temperature around the residential/official construction. Finally, this application is useful as a warning signal throughout this standalone and smart monitoring system for inhabitants through personal devices using the smart mobile phone.

However, more definite conclusions will be possible when the developed system may be helpful in the design of the integrated circuit because the circuit interfaces are capable of optimizing power for miniature generators. Energy storage devices can use this technique to obtain the electrical charge from very-low-power generators. The developed circuit is also suitable for the power consumption of very-small devices using electrical power from other generator sources and future studies.

5.2. Future Prospects

The future work would be possibly developed by following the suggestions of these perspective views just to present the vibration energy harvesting structures which increase the efficiency of this vibration harvesting system and conduct their possibilities of feasible works. Consequently, these studies should investigate the

use of this technology and further optimizations of involved applications regarding to the alternative ways upon the vibration energy harvesting using the piezoelectric method. The needs of their applications are to be concerned within these prospective works as follows:

- The monitoring system omitted human resources accessing or maintaining.
- Very far and dangerous areas for getting and observing their relevant information.
- Daily live using alternative solutions reduced the main energy using for all applications.
- Energy sources as generators for a very-small power consumption corresponding to the continuous and discrete vibrational energy.
- Remote data accessing from inaccessible areas and also real-time monitoring of these harvested structures by using the standalone energy harvesting systems.

At the end of these all sections, these ambition environments would be improved by the previous particular prospects of the piezoelectric material applications to achieve the efficiencies of the alternative energy issues. The expectations for the sustainable requirements of this alternative energy, which are significantly better than other methods. As a result, to further apply these crucial innovations that influence the sustainability based on environmental parameters and their applications undergone by the piezoelectric method and further enhancement circuit for this future prescription as the promising technologies throughout these further works, need to be complete.

REFERENCES

Anderson, M. 2011. Footfalls for Phone Calls - New tech could power portable gadgets with every step [Website Article Version - Research Article], Available from https://spectrum.ieee.org/consumer-electronics/gadgets/footfalls-for-phone-calls. [accessed February 1, 2019].

Arnold, D.P. 2007. Review of Microscale Magnetic Power Generation. IEEE Transactions on Magnetics 43 (11): 3940-3951.

Caliò, R., U.B. Rongala, D. Camboni, M. Milazzo, C. Stefanini, G. De Petris, and C.M. Oddo. 2014. Piezoelectric Energy Harvesting Solutions. Sensors 14 (3): 4755-4790.

Davis, C.L., and G.A. Lesieutre. 1995. A modal strain energy approach to the prediction of resistively shunted piezoceramic damping. Journal of Sound and Vibration 184 (1): 129-139.

Dicken, J., P.D. Mitcheson, S. Member, I. Stoianov, and E.M. Yeatman. 2012. Power-Extraction Circuits for Piezoelectric Energy Harvesters in Miniature and Low-Power Applications. IEEE Transactions on Power Electronics 27 (11): 4514-4529.

Dineva, P.S., D. Gross, R. Müller, and T. Rangelov. 2014. Dynamic Fracture of Piezoelectric Materials - Solution of Time-Harmonic Problems via BIEM, Solid Mechanics and Its Applications. Springer International Publishing: Switzerland.

Erturk, A., and D.J. Inman. 2008. Issues in mathematical modeling of piezoelectric energy harvesters. Smart Materials and Structures 17 (6): 1-14.

Evans, D. 2018. The Internet of Things [Infographic Online and Annual Report]. Cisco Systems, Inc., Available from https://blogs.cisco.com/diversity/the-internet-of-things-infographic. [accessed December 1, 2018].

French, A.P. 1971. Vibrations and Waves, The M.I.T. Introductory Physics Series. W.W. Norton & Company, Inc.: New York, USA.

González, J.L., A. Rubio, and F. Moll. 2002. Human Powered Piezoelectric Batteries to Supply Power to Wearable Electronic Devices. International Journal of the Society of Materials Engineering for Resources 10 (1): 34-40.

Guyomar, D., A. Badel, E. Lefeuvre, and C. Richard. 2005. Toward energy harvesting using active materials and conversion improvement by nonlinear processing. IEEE Transactions on Ultrasonics, Ferroelectrics, and Frequency Control 52 (4): 584-595.

Guyomar, D., C. Richard, A. Badel, E. Lefeuvre, and M. Lallart. 2009. Energy harvesting using non-linear techniques. In: Energy Harvesting Technologies. edited by S. Priya and D.J. Inman. New Tork, USA.: Springer US. 209-266.

IEA. 2018. Air conditioning use emerges as one of the key drivers of global electricity-demand growth [Website Article - Annual Report], Available from https://www.iea.org/newsroom/news/2018/may/air-conditioning-use-emerges-as-one-of-the-key-drivers-of-global-electricity-dema.html. [accessed February 2, 2019].

Ikeda, T. 1990. Fundamentals of Piezoelectricity. Oxford University Press: New York, USA.

Inman, D.J. 2014. Engineering Vibrations. 4th ed. Pearson Education, Inc.: New York, USA.

Jung, H.J., Y. Song, S.K. Hong, C.H. Yang, S.J. Hwang, S.Y. Jeong, and T.H. Sung. 2015. Design and optimization of piezoelectric impact-based micro wind energy harvester for wireless sensor network. Sensors and Actuators A: Physical 222 (2015): 314-321.

Kelly, S.G. 2012. Mechanical Vibrations - Theory and Applications. Cengage Learning Ltd.: Stanford, USA.

Kim, H., S. Lee, C. Cho, J.E. Kim, B.D. Youn, and Y.Y. Kim. 2015. An experimental method to design piezoelectric energy harvesting skin using operating deflection shapes and its application for self-powered operation of a wireless sensor network. Journal of Intelligent Material Systems and Structures 26 (9): 1128-1137.

Krikke, J. 2005. Sunrise for energy harvesting products. IEEE Pervasive Computing 4 (1): 4-5.

Lallart, M., D. Guyomar, Y. Jayet, L. Petit, E. Lefeuvre, T. Monnier, P. Guy, and C. Richard. 2008. Synchronized switch harvesting applied to self-powered smart systems: Piezoactive microgenerators for autonomous wireless receivers. Sensors and Actuators A: Physical 147 (1): 263-272.

Lefeuvre, E., D. Audigier, C. Richard, and D. Guyomar. 2007. Buck-boost converter for sensorless power optimization of piezoelectric energy harvester. IEEE Transactions on Power Electronics 22 (5): 2018-2025.

Lefeuvre, E., A. Badel, C. Richard, L. Petit, and D. Guyomar. 2006. A comparison between several vibration-powered piezoelectric generators for standalone systems. Sensors and Actuators, A: Physical 126: 405-416.

Li, P. 2008. Energy storage is the core of renewable technologies. IEEE Nanotechnology Magazine 2 (4): 13-18.

Mason, W.P. 1935. An Electromechanical Representation of a Piezoelectric Crystal Used as a Transducer. Proceedings of the Institute of Radio Engineers 23: 1252-1263.

Muensit, N., and P. Thainiramit, "Energy Harvesting Circuit Based on Piezoelectric Method for Rechargable Battery,"Prince of Songkla University, Thailand Petty Patent 9240, 21 October, 2014.

Muensit, N., and P. Thainiramit, "Energy Harvesting System Based on Piezoelectric Generator for Rechargable Battery and Electronic Devices,"Prince of Songkla University, Application No.: Thailand Petty Patent 1603002019, Application Date: 5 Oct, 2016.

Ottman, G.K., H.F. Hofmann, A.C. Bhatt, and G.A. Lesieutre. 2002. Adaptive piezoelectric energy harvesting circuit for wireless remote power supply. IEEE Transactions on Power Electronics 17 (5): 669-676.

Ottman, G.K., H.F. Hofmann, and G.A. Lesieutre. 2003. Optimized piezoelectric energy harvesting circuit using step-down converter in discontinuous conduction mode. IEEE Transactions on Power Electronics 18 (2): 696-703.

Raju, M., and M. Grazier. 2010. Energy Harvesting - Ultra Low Power (ULP) Meets Energy Harvesting [Online Report - PDF Document]. Texas Instruments Inc., Available from http://www.ti.com/lit/wp/slyy018a/slyy018a.pdf?DCMP=tmg-issccpr-021712&HQS=issccpr-wp. [accessed December 5, 2018].

Rakbamrung, P., M. Lallart, D. Guyomar, N. Muensit, C. Thanachayanont, C. Lucat, B. Guiffard, L. Petit, and P. Sukwisut. 2010. Performance comparison of PZT and PMN–PT piezoceramics for vibration energy harvesting using standard or nonlinear approach. Sensors and Actuators A: Physical 163 (2): 493-500.

Richard, C., D. Guyomar, and D. Audigier. 1999. *An Original Damping Approach Using A Switched Piezoelectric Device*. Paris, FRANCE: Technomic Publishing Inc.

Richard, C., D. Guyomar, D. Audigier, and G. Ching. 1999. Semi-passive damping using continuous switching of a piezoelectric device. Proc. SPIE 3672: 104-111.

Roundy, S., and P.K. Wright. 2004. A piezoelectric vibration based generator for wireless electronics. Smart Materials and Structures 13 (5): 1131–1142.

Roundy, S., P.K. Wright, and K.S.J. Pister. 2002. Micro-Electrostatic Vibration-to-Electricity Converters. Proceeding of the ASME 2002 International Mechanical Engineering Congress and Exposition Microelectromechanical Systems. at New Orleans, Louisiana, USA, November 17–22, 2002. 487-496.

Roundy, S., P.K. Wright, and J. Rabaey. 2003. A study of low level vibrations as a power source for wireless sensor nodes. Computer Communications 26 (11): 1131-1144.

Sodano, H.A., D.J. Inman, and G. Park. 2004. A review of power harvesting from vibration using piezoelectric materials. Shock and Vibration Digest 36 (3): 197-205.

Sodano, H.A., D.J. Inman, and G. Park. 2005. Comparison of Piezoelectric Energy Harvesting Devices for Recharging Batteries. Journal of Intelligent Material Systems and Structures 16 (10): 799-807.

Tan, Y.K. 2013. Energy Harvesting Autonomous Sensor Systems : Design, Analysis, and Practical Implementation. CRC Press Taylor & Francis Group: New York.

Tan, Y.K., K.Y. Hoe, and S.K. Panda. 2006. Energy Harvesting using Piezoelectric Igniter for Self-Powered Radio Frequency (RF) Wireless Sensors. Proceeding of the Industrial Technology, 2006. ICIT 2006. IEEE International Conference on. at Mumbai, India, 15-17 Dec. 2006. 1711-1716.

Thainiramit, P. 2012. Developments of Energy Harvesting Using the Piezoelectric Methods. Master Thesis, Department of Physics, Faculty of Science, Prince of Songkla University.

Thomson, W.T. 1993. Theory of Vibration with Applications. 4th ed. Springer Science & Business Media, Inc.: New York, USA.

Torah, R., P. Glynne-Jones, M. Tudor, T. O'Donnell, S. Roy, and S. Beeby. 2008. Self-powered autonomous wireless sensor node using vibration energy harvesting. Measurement Science and Technology 19 (12): 1-8.

Vahid, F., and T. Gevargis. 2002. Embedded System Design : A unified Hardware / Software Introduction. John Wiley & Sons (Asia) Pte. Ltd.: Kundli, India.

Williams, C.B., and R.B. Yates. 1996. Analysis of a micro-electric generator for microsystems. Sensors and Actuators, A: Physical 52 (1-3): 8-11.

VITAE

Name Mr. Panu Thainiramit

Student ID 5610930021

Education Attainment

Degree	Name of Institution	Year of Graduation
Master of Science (Physics)	Prince of Songkla University	2013
Bachelor of Engineering (Computer)	Walailak University	2008

Work – Position and Address

April 2018 – July 2018: Lecturer of Renewable Energy Technology Program, Faculty of Sciences Technology and Agriculture. Yala Rajabhat University, Thailand.

List of publications and Proceedings

Thainiramit, P., Y. Wahab, M.Z. Mohd Zin, E. Saniso, K. Techato and N. Muensit. 2019. Development of a Technique for Energy Storage Using a Piezoelectric Generator for Low-Power Consumption Devices Supporting Stand-Alone Wireless Sensors for Smart Systems. The International Journal of Integrated Engineering (IJIE) Vol.11, No.1: Page(s) 39-44.

Thainiramit, P., Y. Wahab, K. Techato, P. Sukwisute and N. Muensit. 2019. Excited Discrete Force for Piezo generator Undergone Ultra-Low Vibrations on Air-Compressor and Possible Application. International Conference 2019 IEEE 15th International Colloquium on Signal Processing & its Application (CSPA 2019): Page(s) 48-53, 8th - 9th March 2019. PARKROYAL Penang Resort Batu Ferringhi Beach 11100 Penang MALAYSIA.

VITAE (cont.)

List of Petty-Patents

Muensit, N., and P. Thainiramit, "Energy Harvesting Circuit Based on Piezoelectric Method for Rechargable Battery,"Prince of Songkla University, Thailand Petty Patent 9240, 21 October, 2014.

Muensit, N., and P. Thainiramit, "Energy Harvesting System Based on Piezoelectric Generator for Rechargable Battery and Electronic Devices,"Prince of Songkla University, Application No.: Thailand Petty Patent 1603002019, Application Date: 5 October, 2016.

Awards

The Best Paper Award, in 2019 IEEE 15th International Colloquium on Signal Processing & its Application (CSPA 2019), 8th – 9th March 2019. PARKROYAL Penang Resort Batu Ferringhi Beach 11100. Penang, MALAYSIA.